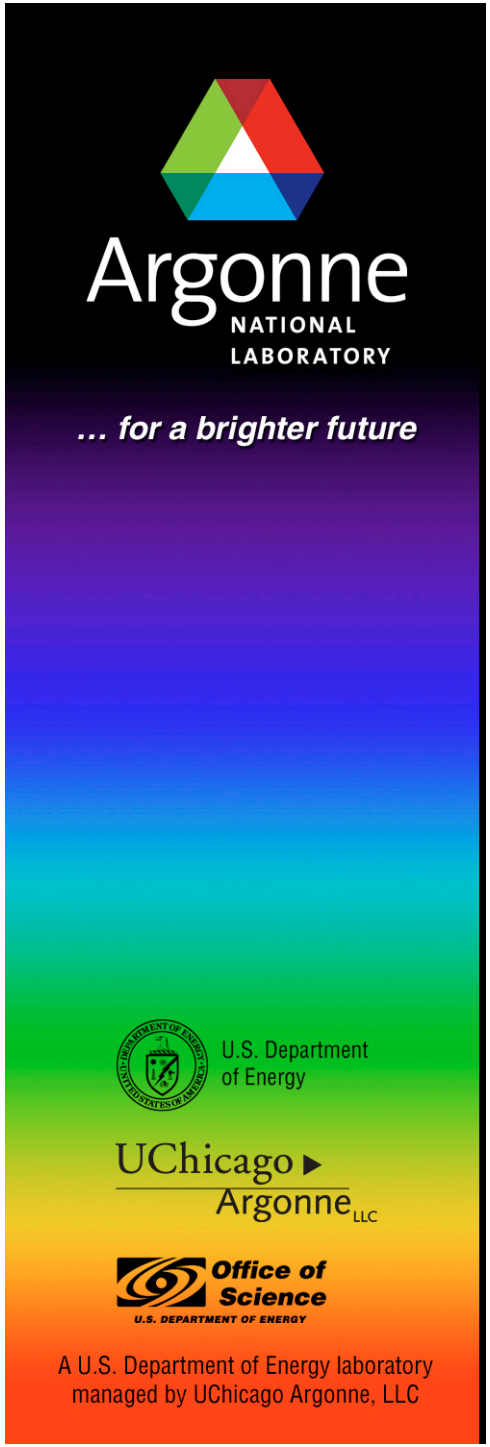

High Energy X-rays Applications

Dean R. Haeffner

Advanced Photon Source

Argonne National Laboratory

Presented at the

National School for Neutron and X-ray Scattering

June 9, 2009

High Energy X-rays?

Loose definition ➪
- Photons between 40 - 120 keV

Why?

Low Absorption
- Bulk measurements
- Special environments
  - *Furnaces*
  - *Reaction cells*
  - *Cryostats*
  - *High-pressure cells*
- Often comparable to neutrons

Simplified Scattering
- Kinematical diffraction
- Small absorption, polarization, & dispersion corrections

Small Diffraction Angles
- Large Q range
- Forward scattering

What?

Stress/strain/texture measurements

Small-angle scattering

High energy diffraction microscopy (HEDM)
- (i.e., grain tracking)

Pair distribution functions (PDF)
- Includes high-pressure

Powder diffraction
- High-resolution (point counting)
- Time-resolved (area detectors)

Diffuse scattering

Triple-axis diffractometry

Fluorescence measurements

Imaging
- Tomography
- Radiography

Combinations of the above
- SAXS/WAXS
- Imaging/WAXS

X-ray Absorption

$$I_x = I_o e^{(\mu/\rho)\rho x}$$

I_o	original beam intensity
I_x	measured beam intensity
μ/ρ	mass absorption coeff.
ρ	material density
x	material thickness

$$\mu_{pe} \sim Z^3 / E^3$$

Note: Compton scattering becomes increasing more important as Z decreases and E increase.

Photon Mass Absorption for Fe

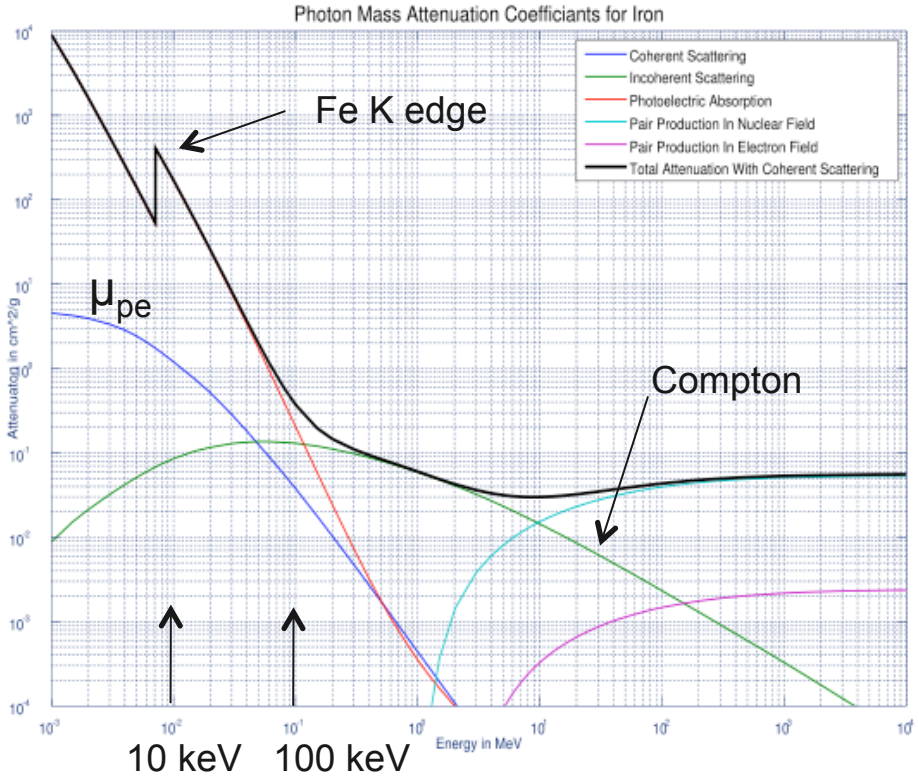

Graph form wikipedia

X-ray Absorption at High Energies

Low Absorption
- Bulk measurements
- Smaller absorption corrections to data
- Special environments
  - *Furnaces*
  - *Reaction cells*
  - *Cryostats*
  - *High-pressure cells*

Often comparable to neutrons

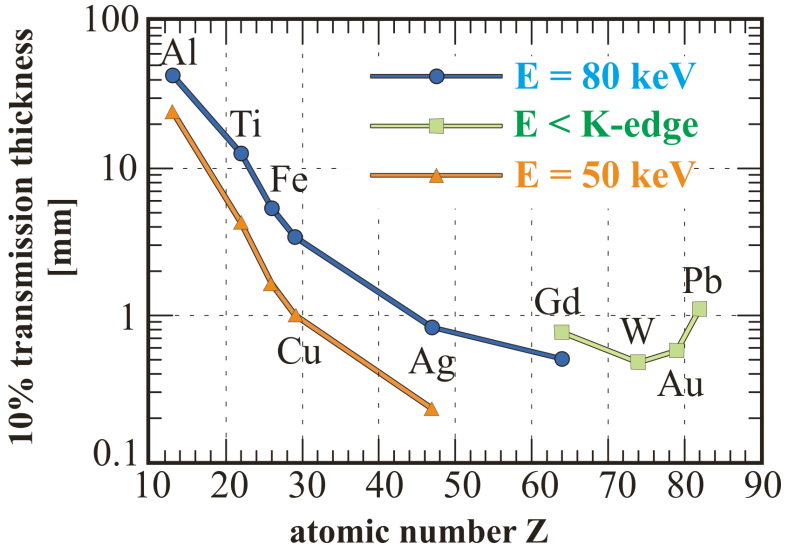

X-ray Penetration Distances in Selected Metals

Material	Mo tube 17.48 keV	Synchrotron, 80 keV
Copper	0.10 mm	6.9 mm
Bronze (10%Sn)	0.11 mm	5.5 mm
Brass (25%Zn)	0.11 mm	7.1 mm
Wrought Iron (0.01 % C)	0.16 mm	10.7 mm
Cast Iron (3 % C)	0.17 mm	11.2 mm

Simplified Scattering

- More kinematical scattering
  - Extinction length ~ E
  - Dynamical scattering $I \sim |F|$
  - Kinematical scattering $I \sim |F|^2$
  - In between is a problem
    - *Primary/secondary extinction*

- Smaller diffraction angles lead to smaller polarization effects

- For all but heavy elements, well above the K-edges
  - Cerium K-edge at 40.44 keV
  - Negligible anomalous scattering effects for most cases

Forward Scattering/High Q

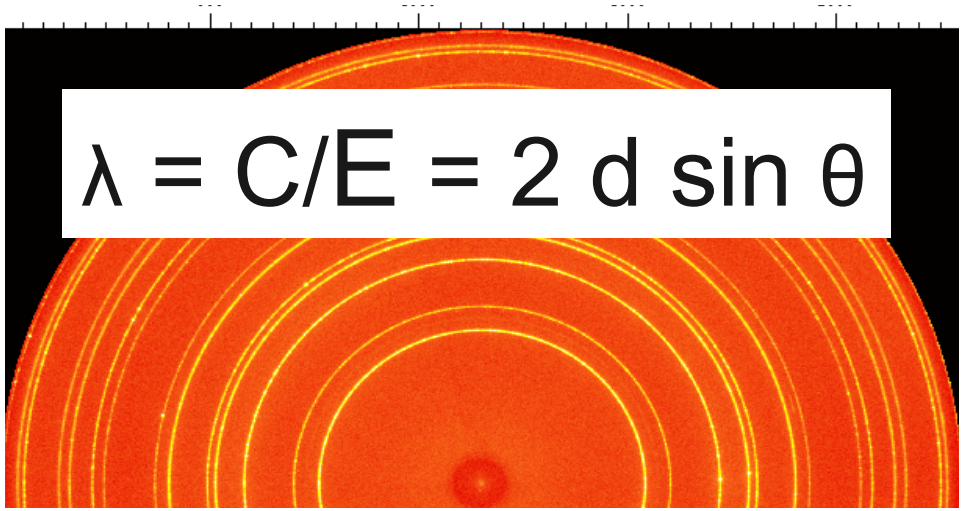

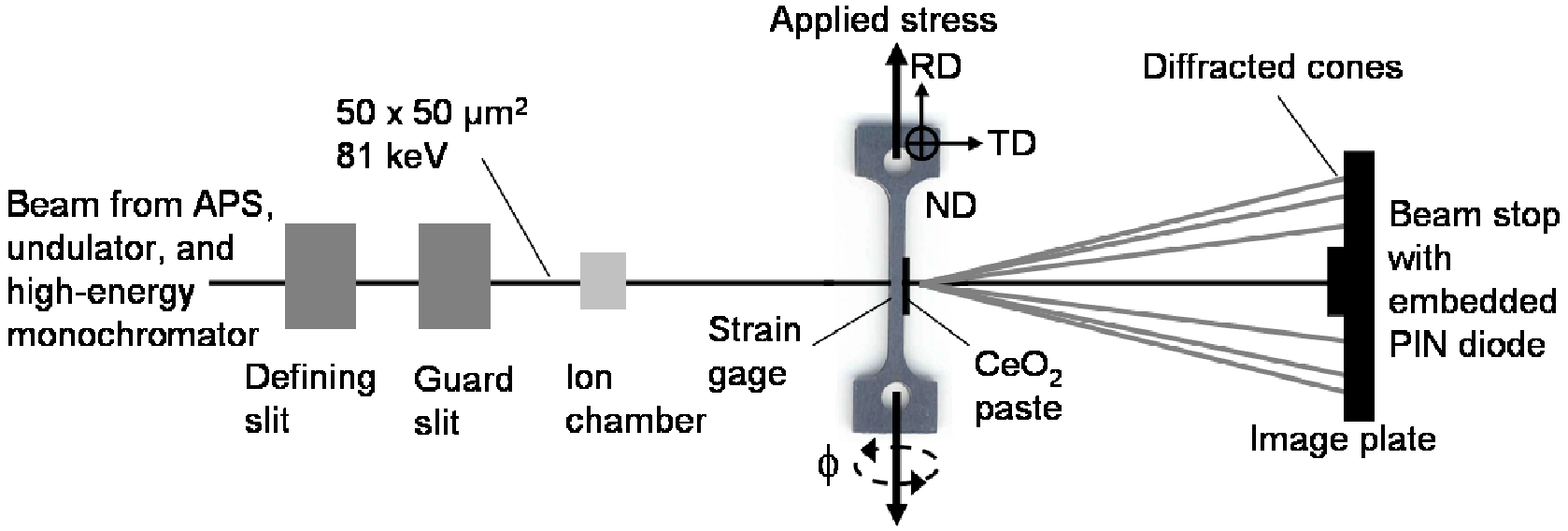

Where Do We Find High-Energy X-rays

High Energy,
Third Generation
Synchrotrons

Brilliance of Various Sources

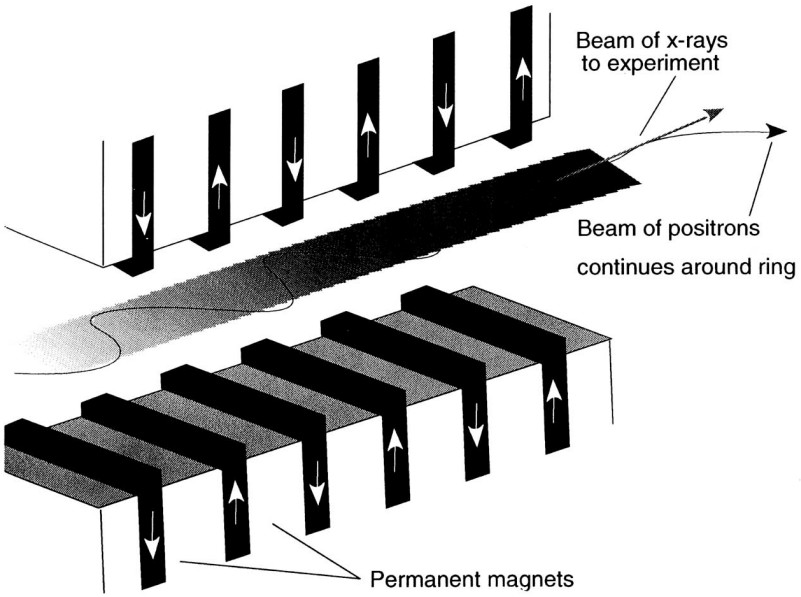

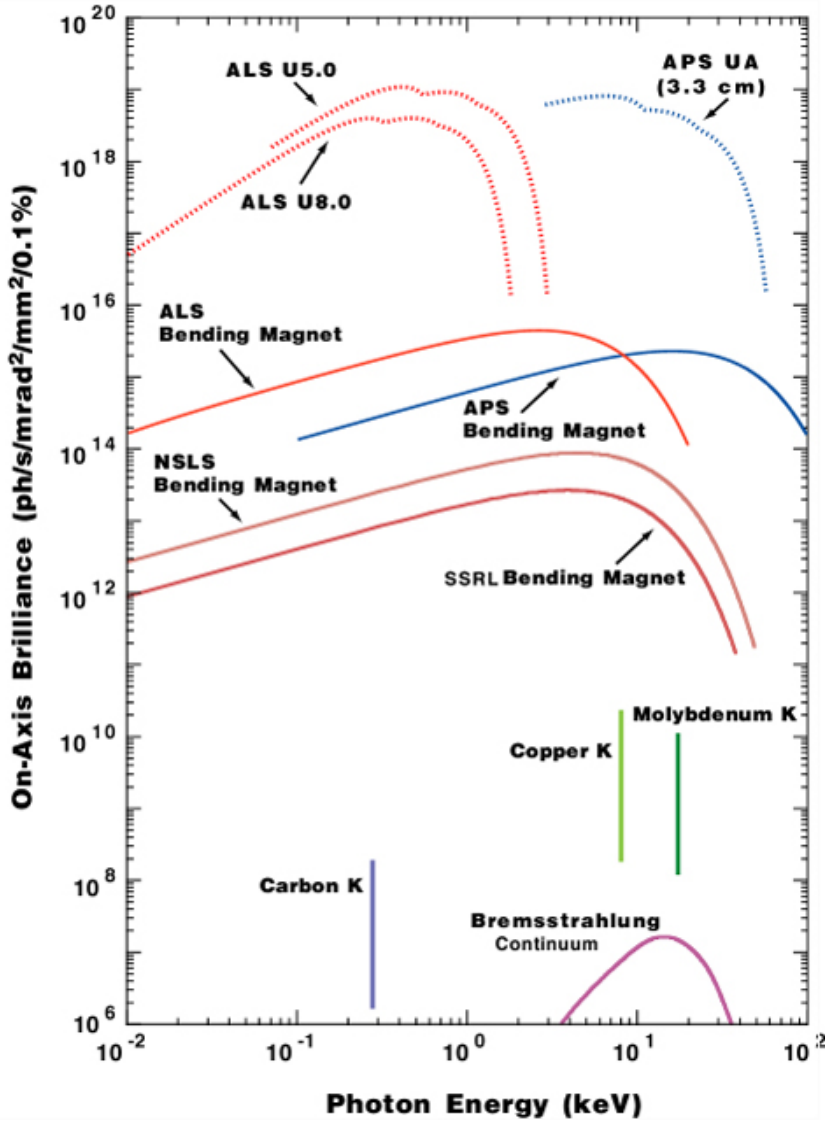

Brilliance of Various Sources

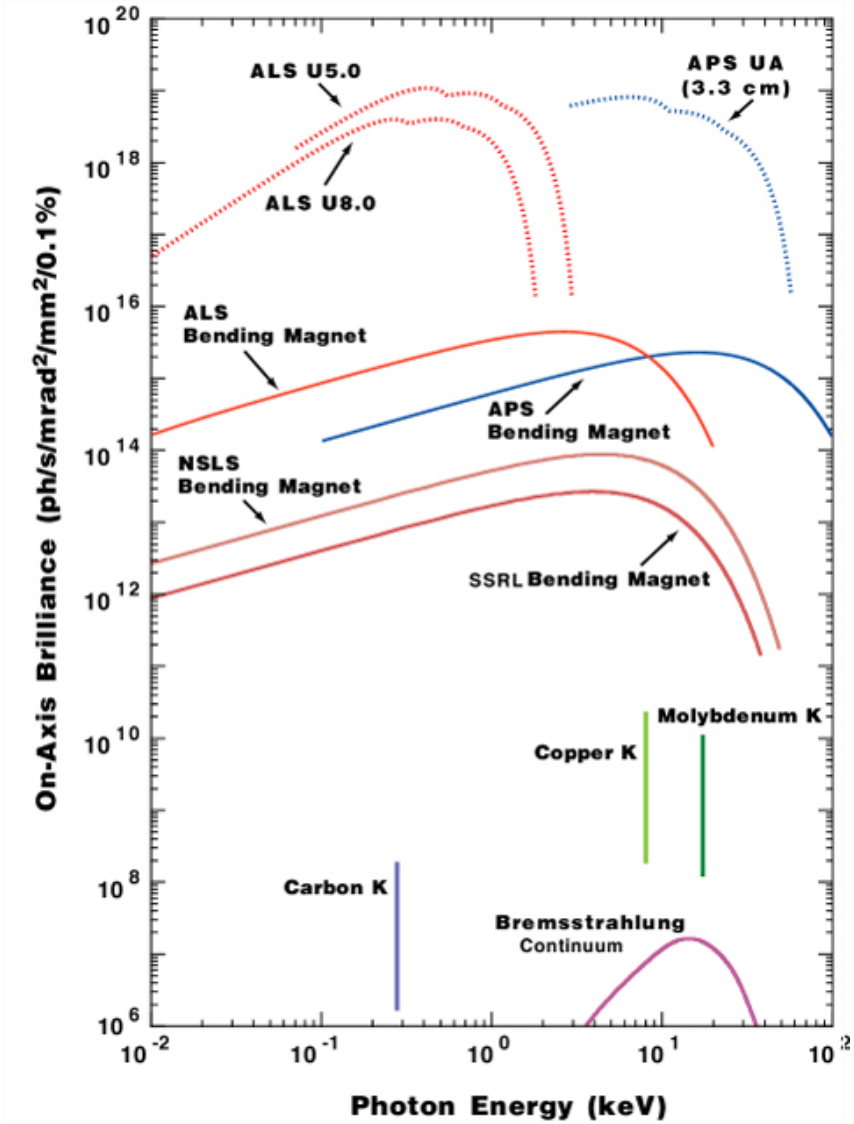

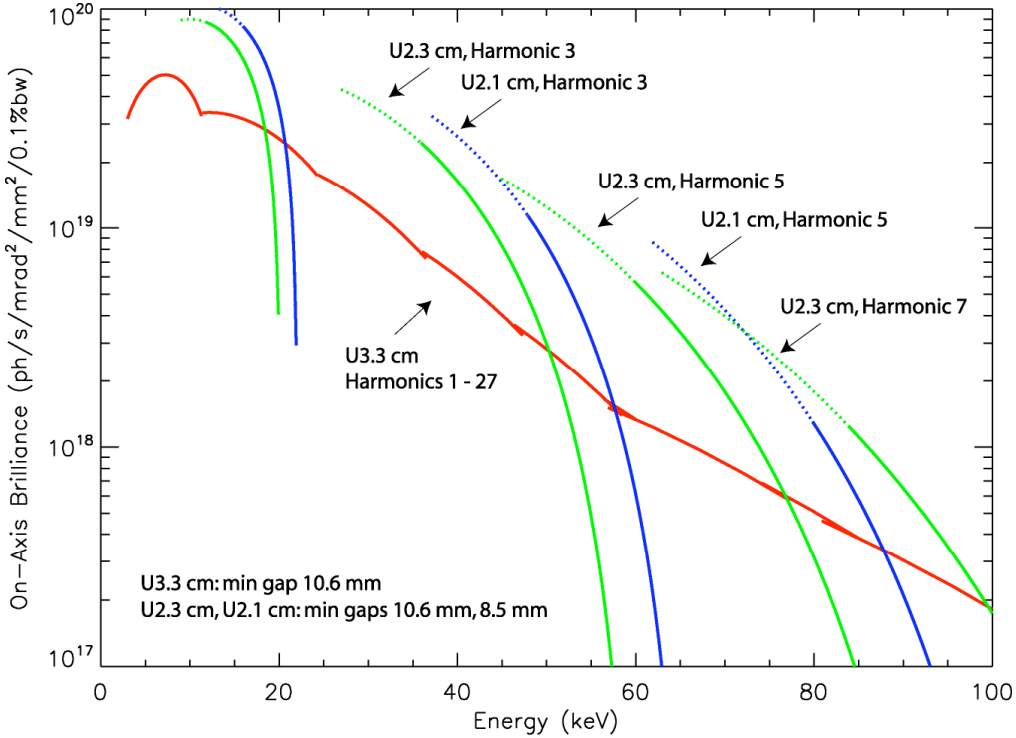

The Future Is Bright

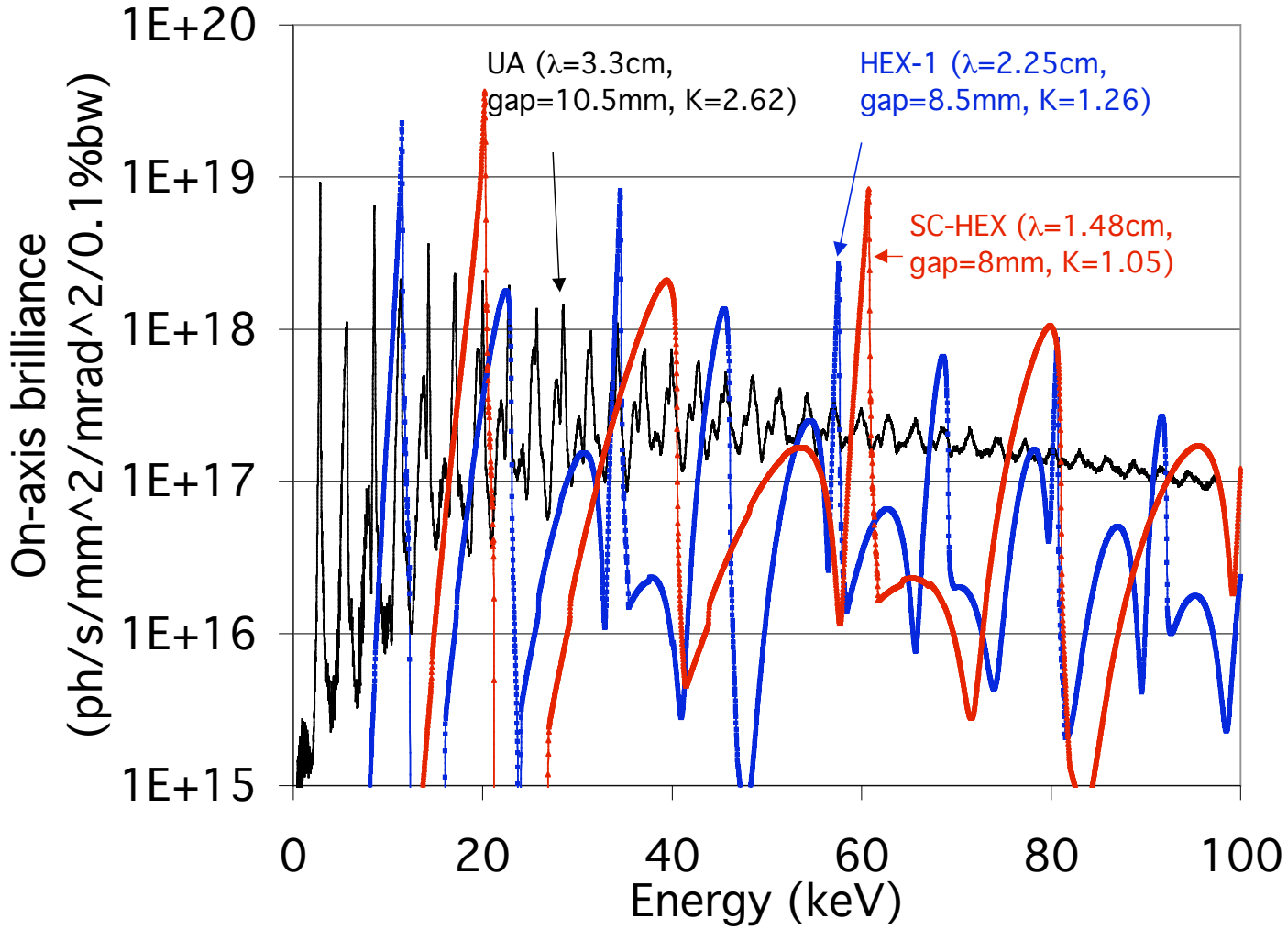

APS High Energy Beamlines

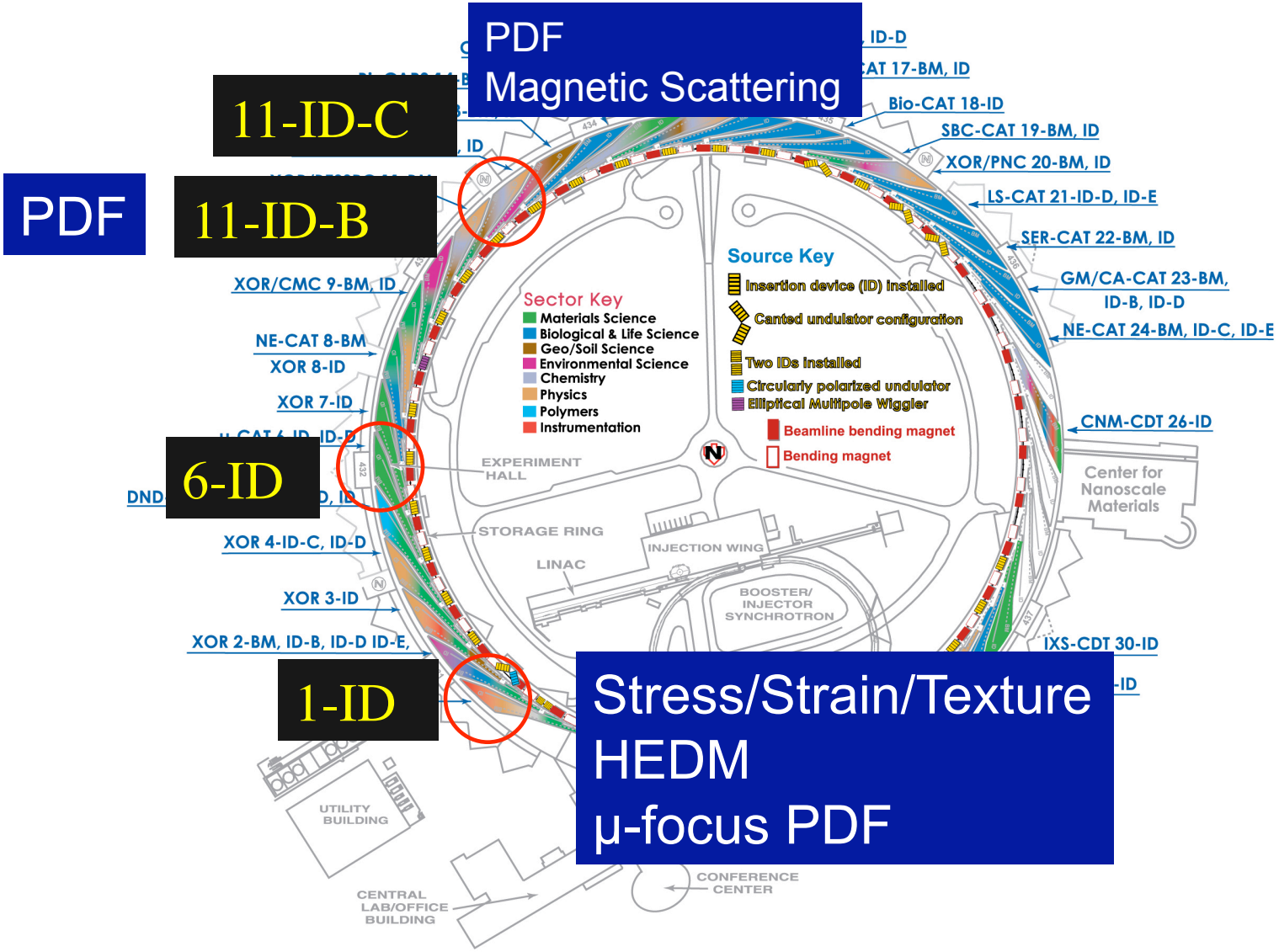

DuMond diagram of flat crystals

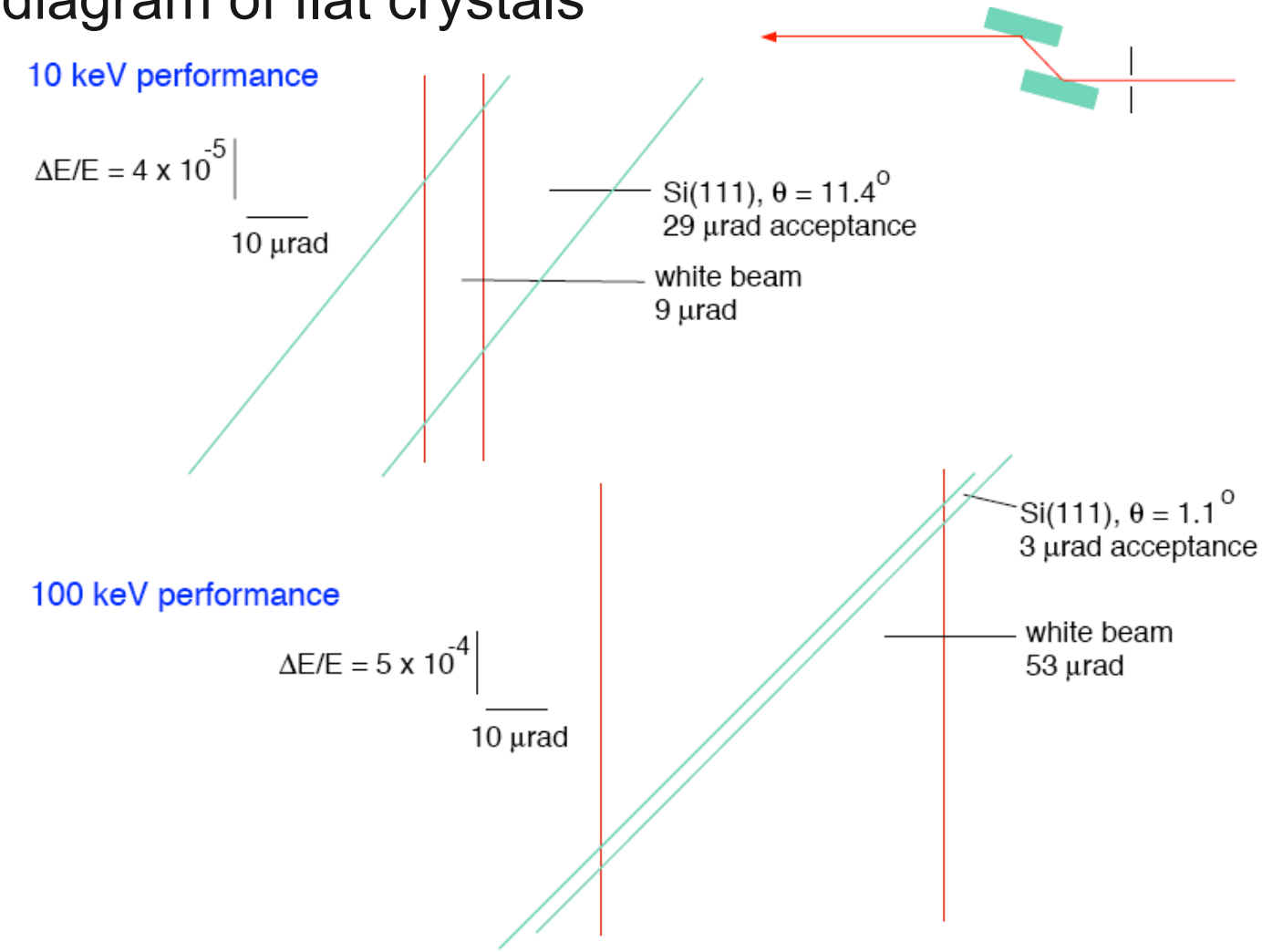

High Energy X-ray Optics at 1-ID

- I-ID Optics
  - Fully tunable 45 to 120 keV
  - Brilliance preserving optics
  - Compound optics
    - *Focusing*
      - ~2 μm possible
      - 20 μm typical
    - *High energy resolution*
      - Resonant scattering
      - Other applications needing better energy resolution

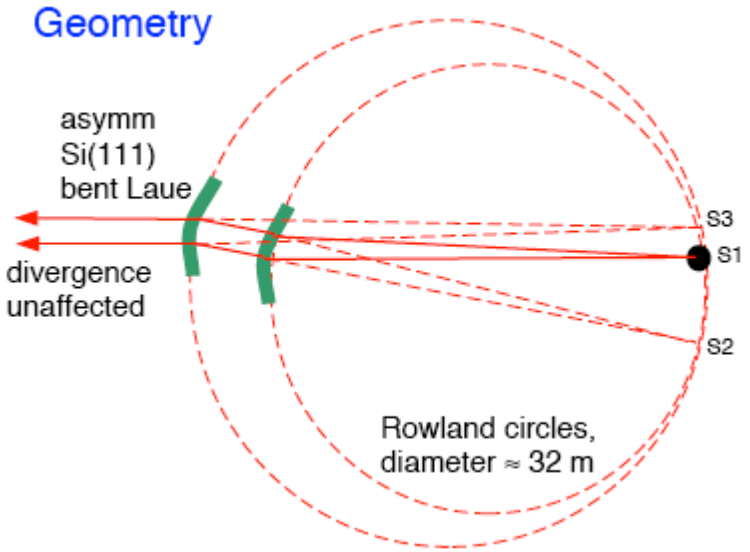

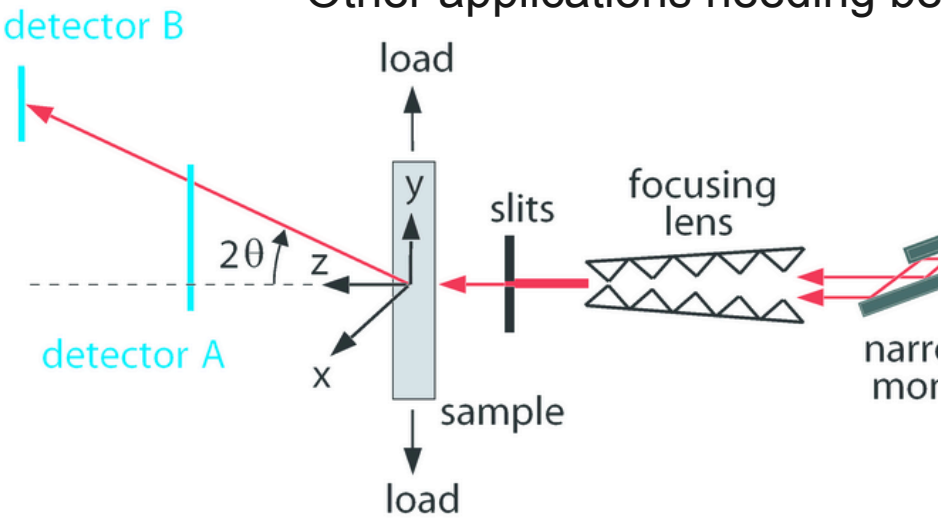

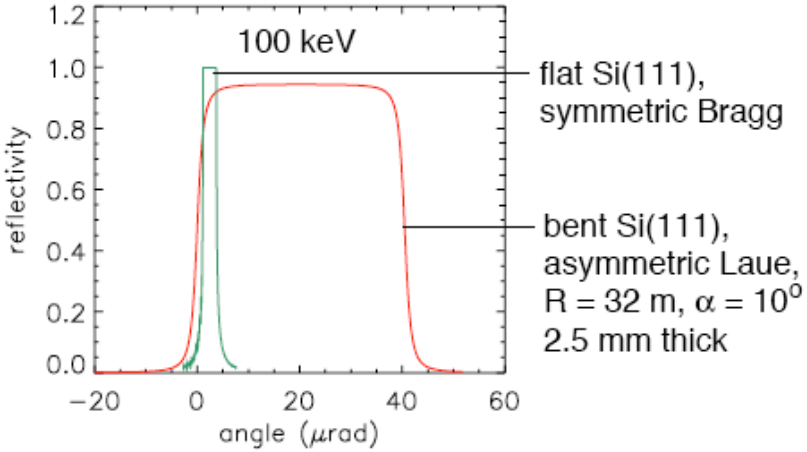

Special Environments

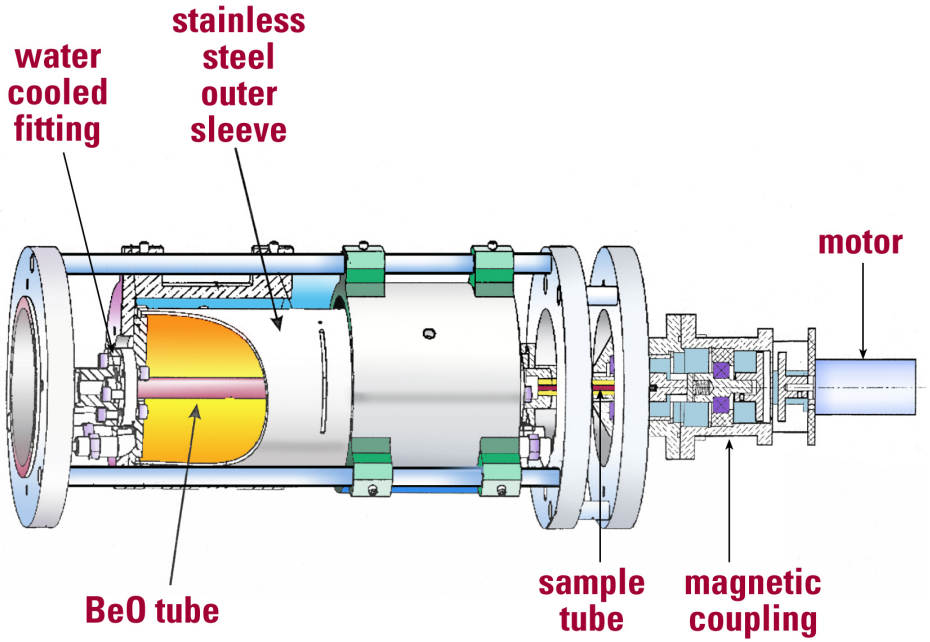

Kramer, Margulies, McCallum, Zhao, Goldman, Lee, & Haeffner

Detectors

Bruker 6500 CCD

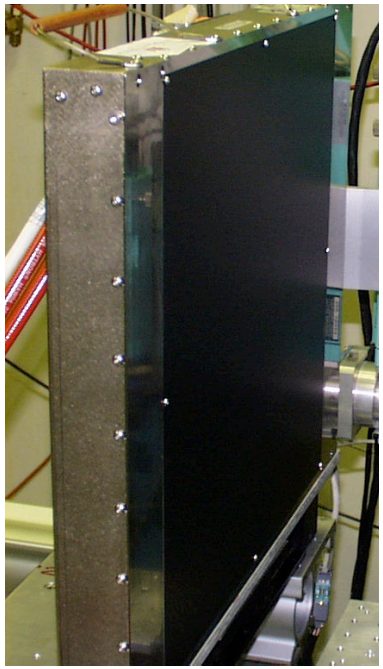

GE Rad detector

Mar345 on-line image plate

Example 1: Aggregate Stress/Strain/Texture

1. ***Powder limit: N > ~1000***
   - Average strain and orientation distribution (texture).
   - *Useful* if gradients » grain size.
   - Well-established techniques (esp. for surface: $\sin^2\psi$ method).

2. ***Finite N***
   - Grain boundary mapping, intragranular stress, local texture: "Grain-boundary engineering"
   - Test local deformation models.
   - Emerging techniques...

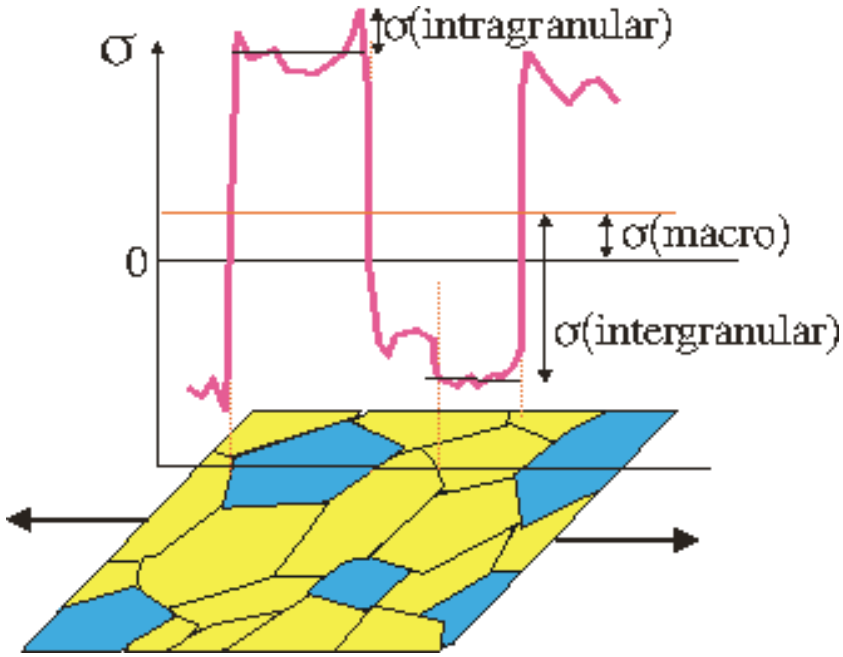

Absolute scale —

0.01 - 1000 μm

Nanoscience - Engineering

Local Strain and Texture Mapping with High-Energy X-rays

SR Property	Enables	Scale	Science
High-energies	High-penetration depths	many mm.	Bulk studies/complicated environments
Low emittance & high flux	Spatial resolution	μm	Local strains&texture
High flux (& area detectors)	Temporal resolution	(sub)sec.	Phase transitions, strain relaxation

Strain is measured with diffraction using Bragg's law

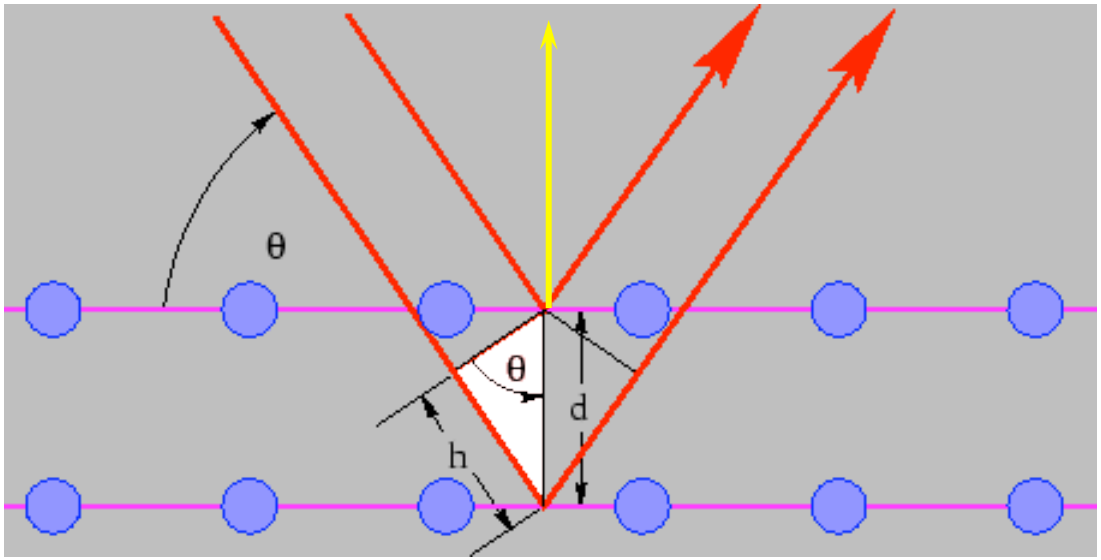

$$\lambda = 2d\sin\theta$$

$$\varepsilon = \frac{d - d_o}{d_o} = \frac{\sin\theta_o}{\sin\theta} - 1$$

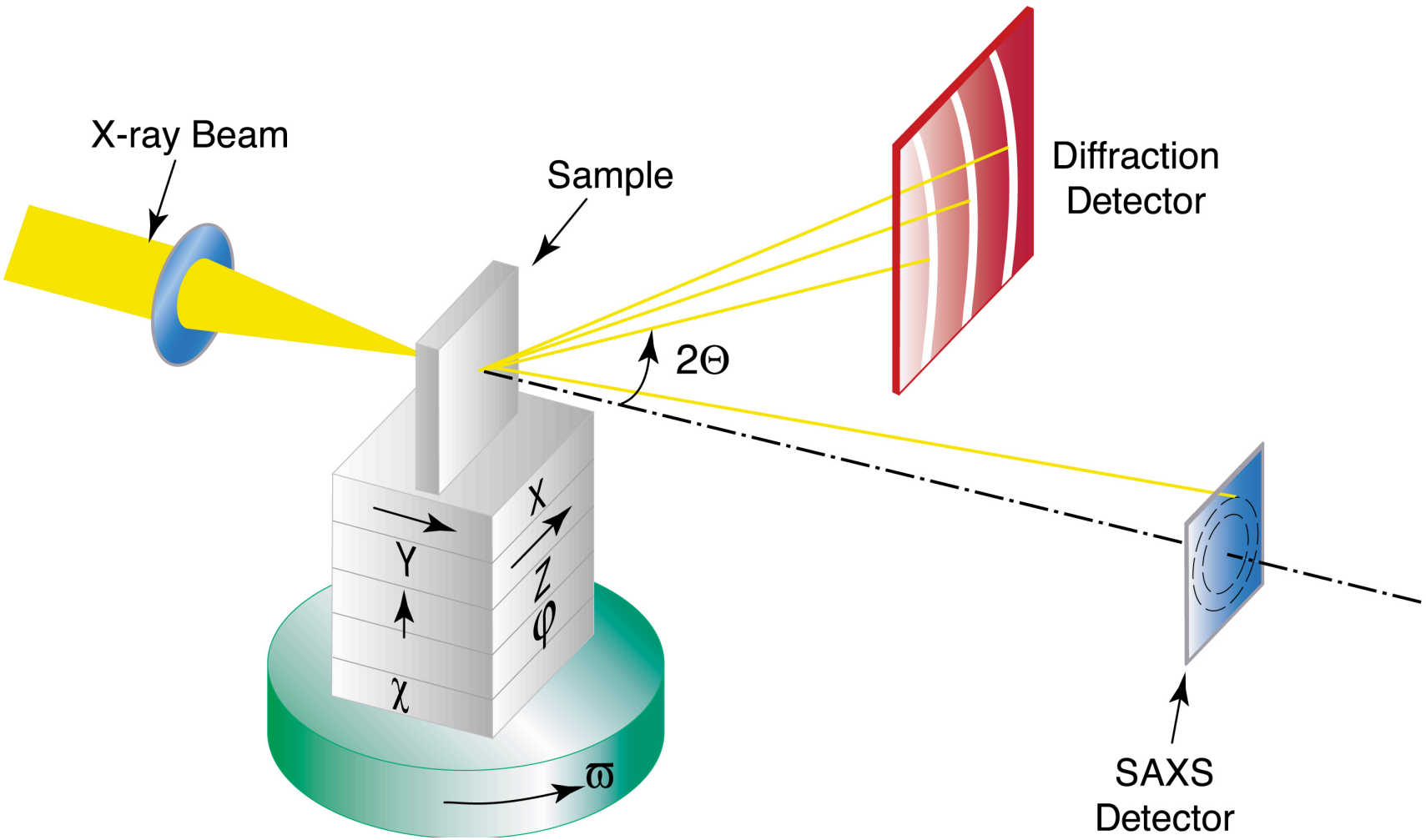
X-ray Beam
Sample
Diffraction
Detector
2Θ
X
Y
Z
φ
χ
ω
SAXS
Detector

Load Partitioning in Ultrahigh Carbon Steel (UHCS)

Marcus Young (Northwestern/ANL), Jon Almer, Ulrich Lienert (APS), David Dunand (Northwestern), Oleg Sherby (Stanford)

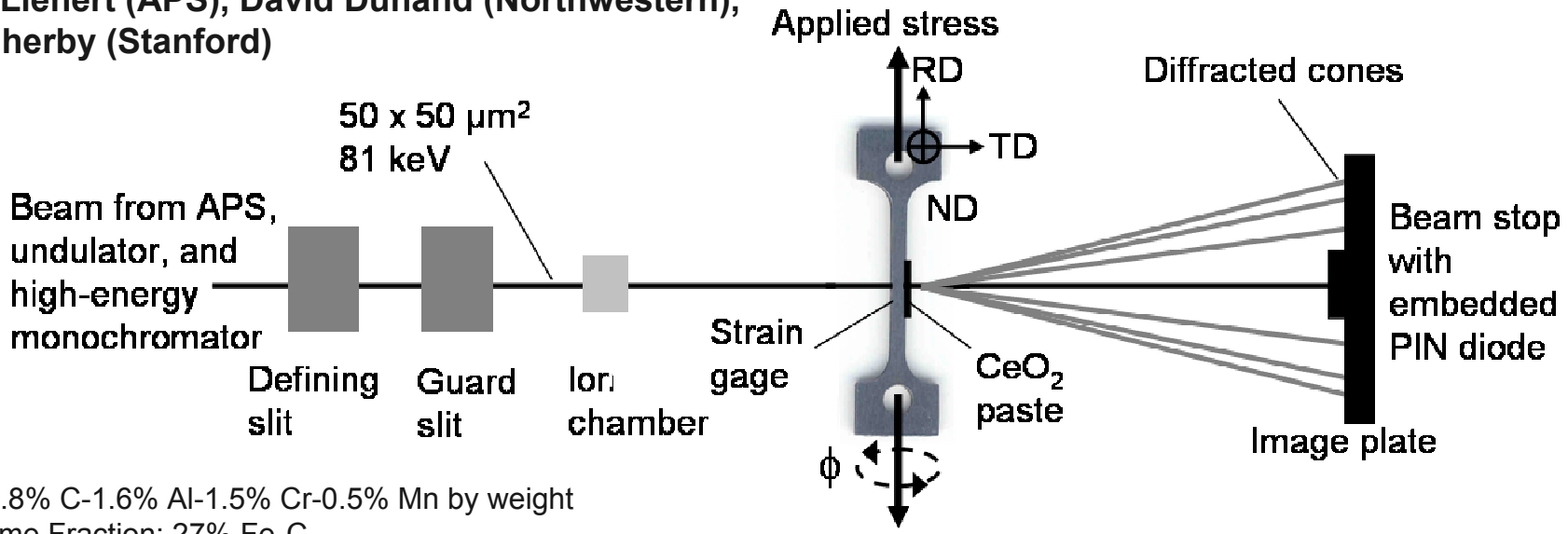

- Fe-1.8% C-1.6% Al-1.5% Cr-0.5% Mn by weight
- Volume Fraction: 27% Fe_3C
- Processing:
  - Soaked at 1093 °C for 8 hrs
  - Hot-rolled in several steps from 1093 °C to 900 °C
  - Hot-sheared into segments
  - Soaked at 1093 °C for 48 hrs & furnace-cooled
  - Reheated to 810 °C
  - Warm-rolled continuously to 750 °C
  - Additional Anneal:
    - *Held at 200 °C for 1 hr*
    - *Heated to 950 °C for 20 min in vacuum furnace*
    - *Furnace cooled*

UHCS Macro- and Micro-Data upon Loading

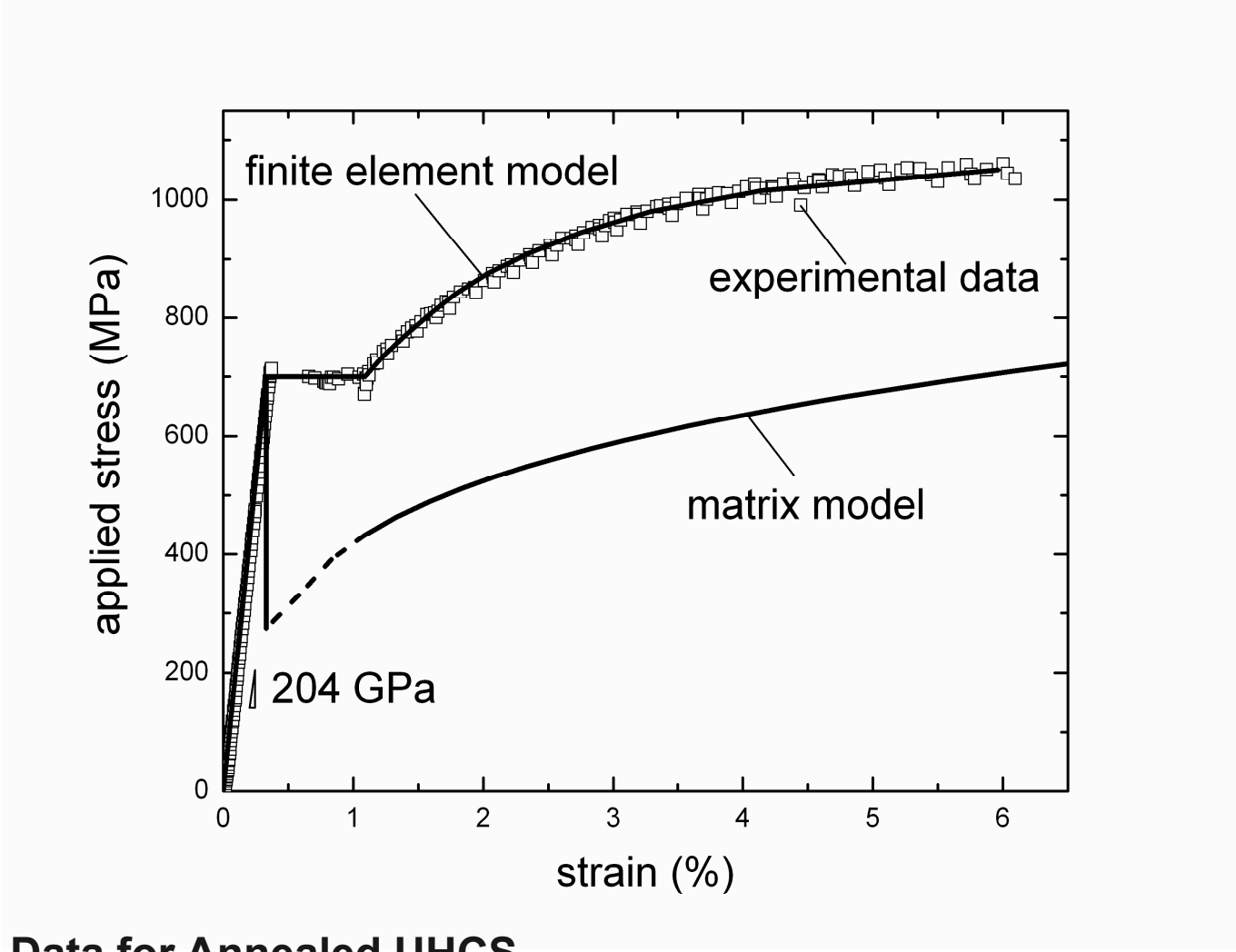

Macro-Data for Annealed UHCS

A Typical X-ray Diffraction Pattern for UHCS

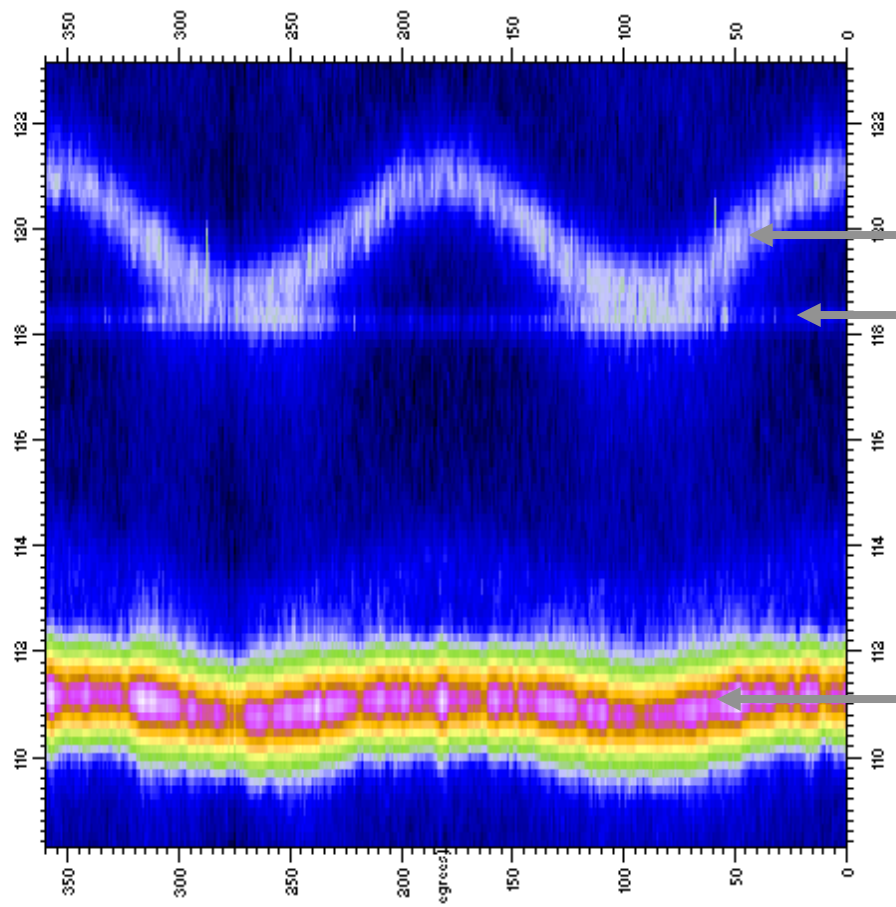

Radial Distance (mm)

σ_{app} = 1035 MPa

Fe_3C (123)

CeO_2 (400)

Fe (200)

Strain Development & Strain-Free Point

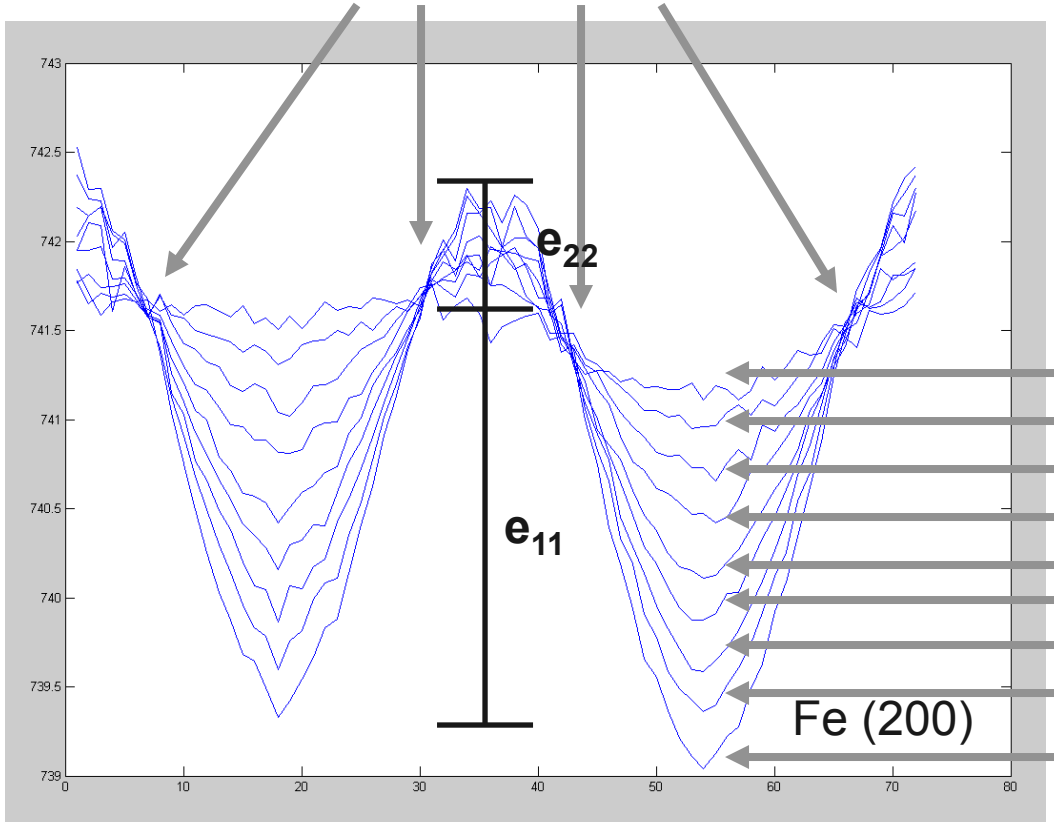

$$\nu \cong \frac{e_{22}}{e_{11}}$$

σ_{app} = 3.5 MPa
σ_{app} = 29 MPa
σ_{app} = 79 MPa
σ_{app} = 130 MPa
σ_{app} = 189 MPa
σ_{app} = 254MPa
σ_{app} = 305 MPa
σ_{app} = 360 MPa
σ_{app} = 416 MPa

UHCS Annealed Micro-Data upon Loading

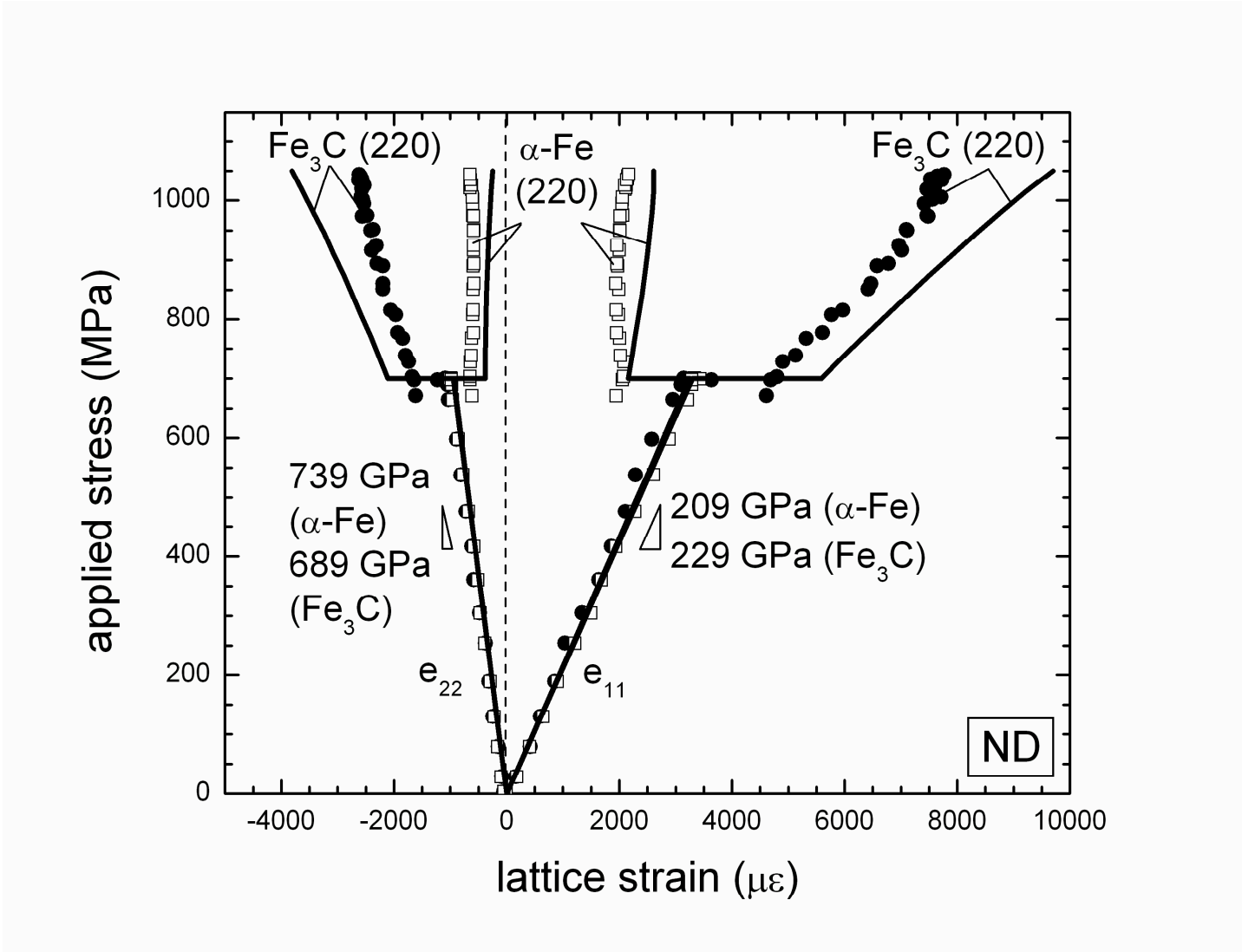

UHCS Annealed Micro-Data upon Loading

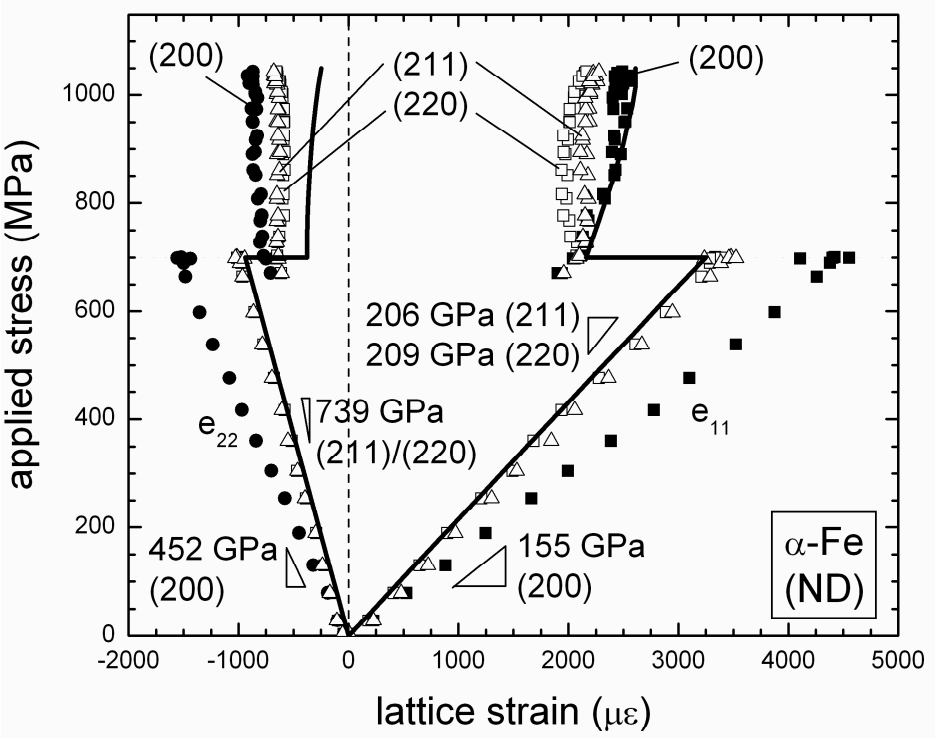

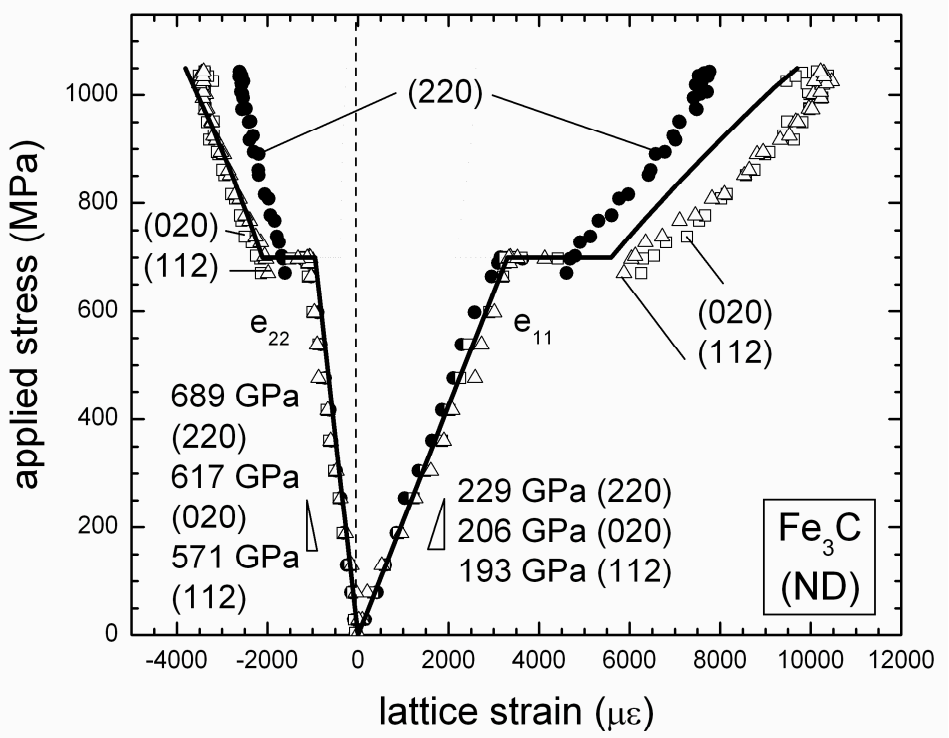

M.L. Young, J.D. Almer, M.R. Daymond, D.R. Haeffner, D.C. Dunand, "Load partitioning between ferrite and cementite during elasto-plastic deformation of an ultrahigh-carbon steel," Acta Mater. 55 (6), 1999-2011 (2007).

Biomechanics of Bone and Teeth

Collaboration with Jon Almer (APS), S. Stock, D. Dunand, C. Brinson, several students (Northwestern Univ.)

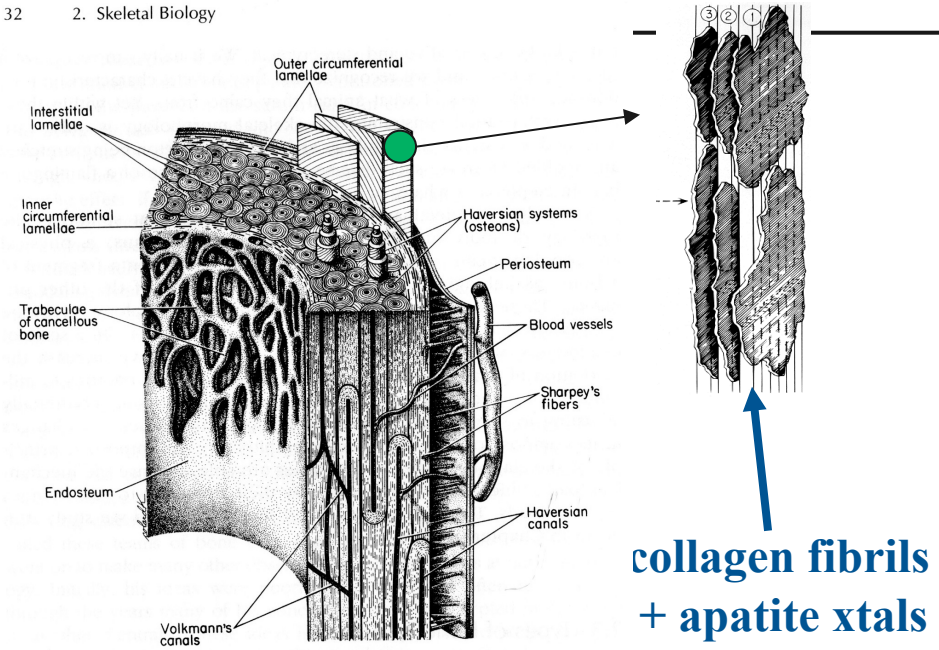

FIGURE 2.1. Sketch of some important features of a typical long bone. (After Benninghoff, 1949.)

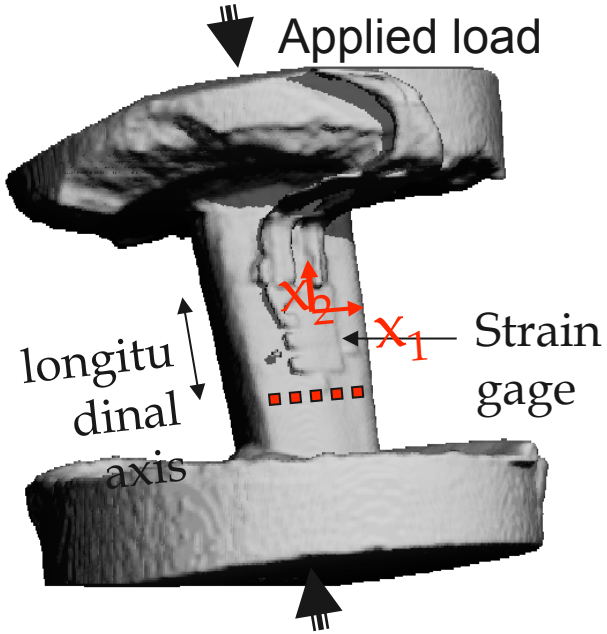

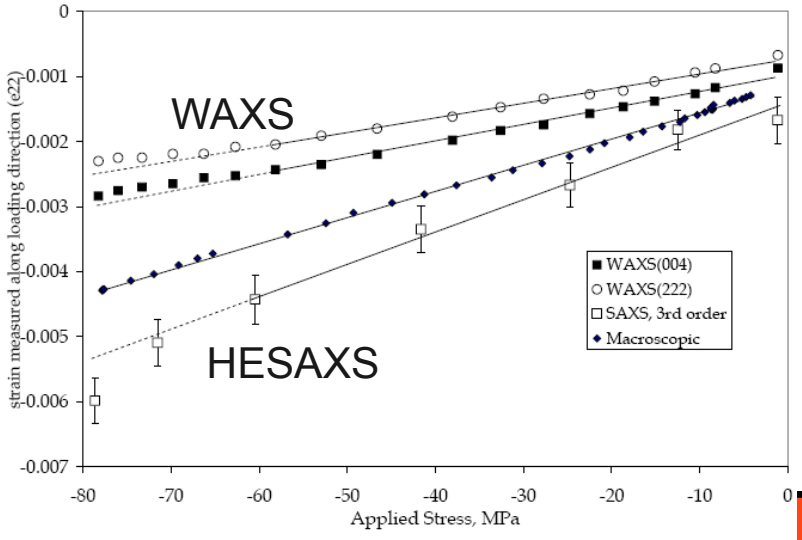

Example 2: High Energy Diffraction Microscopy (HEDM)

1. ***Powder limit: N > ~1000***
   - Average strain and orientation distribution (texture).
   - *Useful* if gradients » grain size.
   - Well-established techniques (esp. for surface: $\sin^2\psi$ method).

2. ***Finite N***
   - Grain boundary mapping, intragranular stress, local texture: "Grain-boundary engineering"
   - Test local deformation models.
   - Emerging techniques...

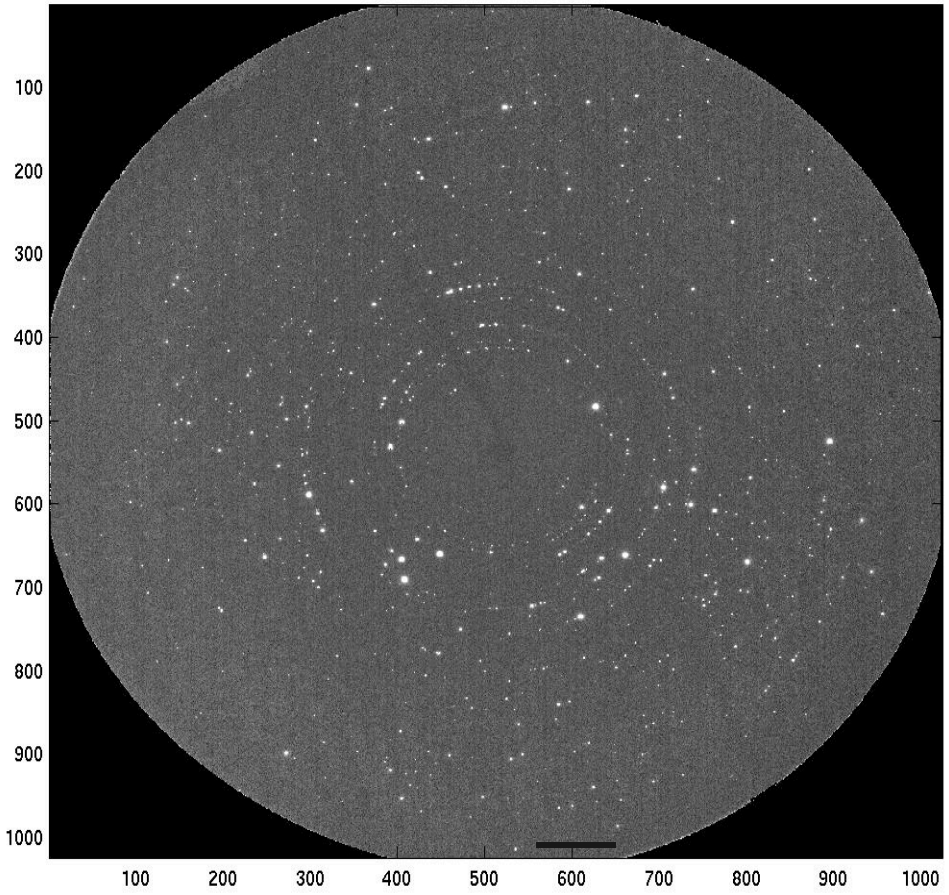

Coarse-grained material

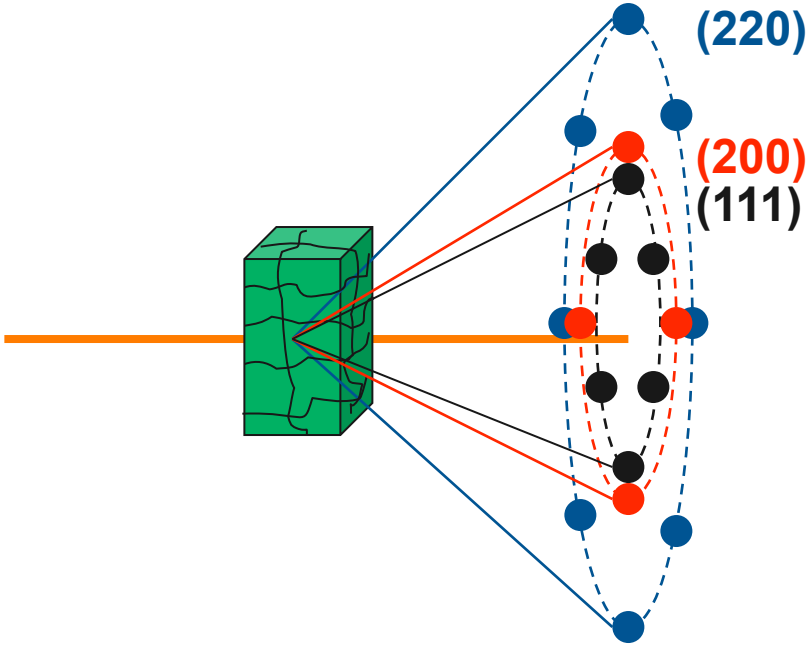

Fine-grained material

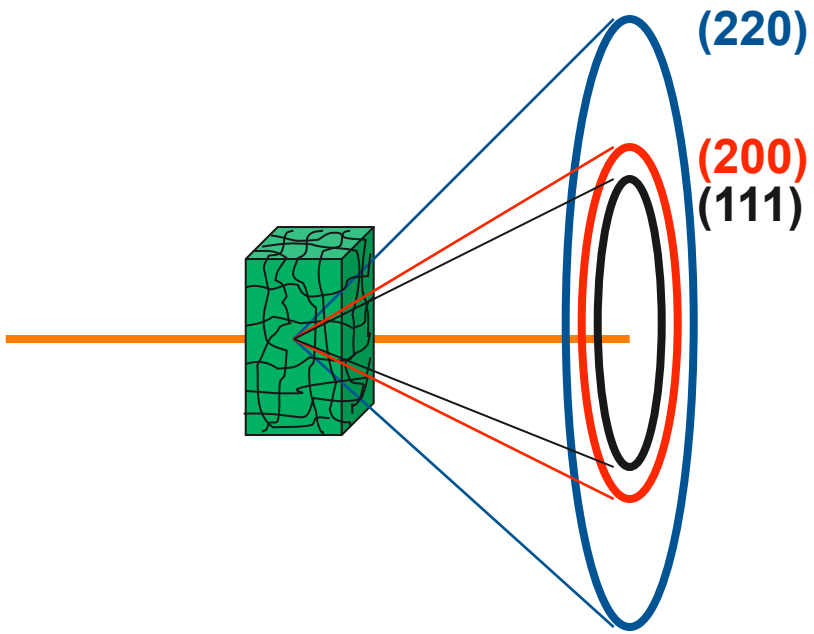

High Energy Diffraction Microscopy (HEDM)

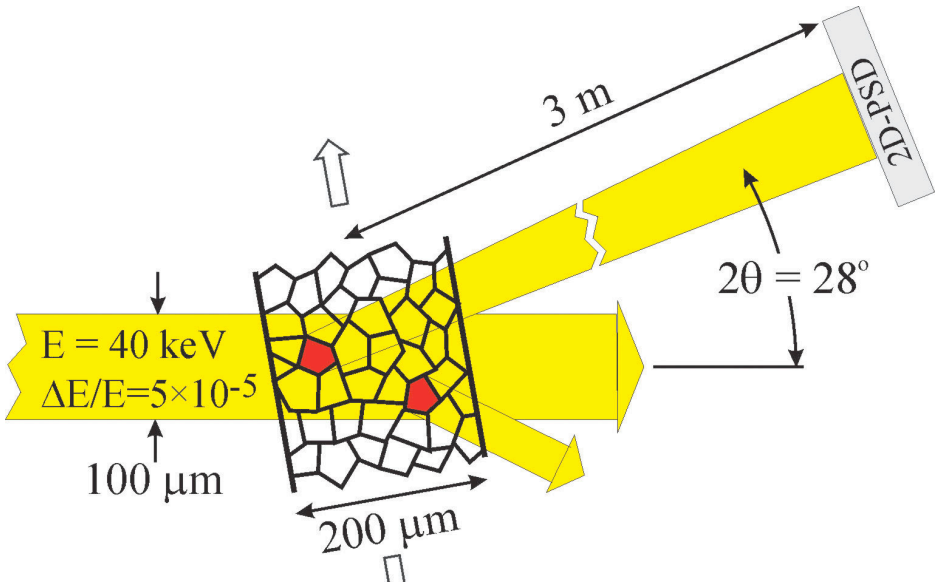

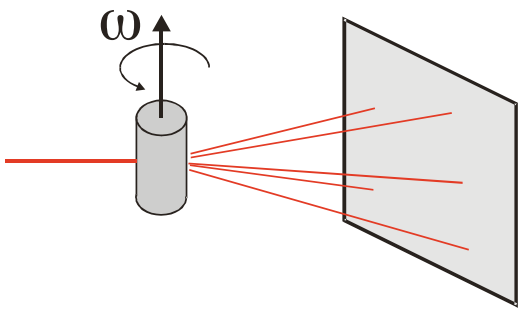

- Several Modes
  - Far field, medium q resolution
    - *Grain rotation during deformation*
  - Far field, high q resolution
    - *Dislocations cells & subgrain structure in Cu*
  - Tracking
    - *Grain topography*
    - *Anomalous grain growth in Al*

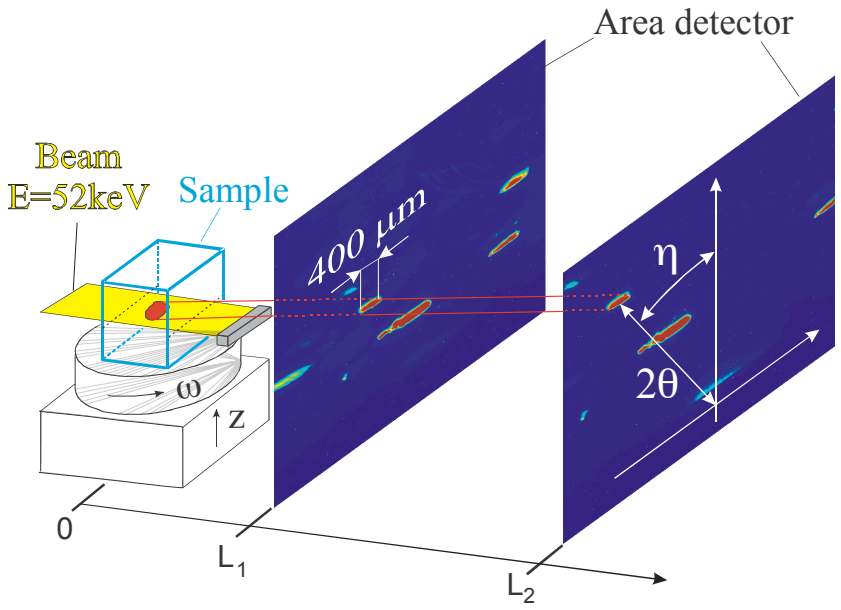

Ulrich Lienert
Risø
Suter Group, Carnegie Mellon

High Energy Single Grain Diffraction

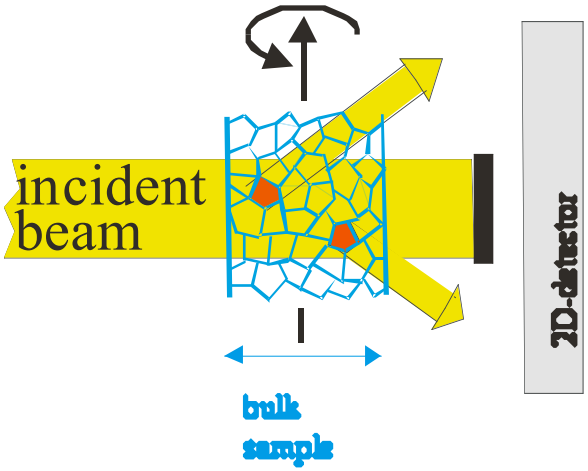

- Orientation contrast
- Small scattering angles
- Intensity ∝ volume
- 'parallel' data acquisition
- Multigrain indexing software
- Spot overlap
  - Linear in number of domains
  - Quadratic in orientation spread

Near field

- Position dominates strain
- Diffracted beams project grain outline

Far field

- strain dominates position
- 'sensitivity': < 0.1 mm (signal-to-noise)
- Spatial information: 'box scan'

High Resolution Reciprocal Space Mapping

Aim:
Characterization of evolving dislocation structure during plastic deformation:

Cell formation?
Subdivision?
Stability?
Strain?

Samples:
FCC metals, tensile deformation up to 4.5%

Experiment:
In-situ, bulk single grain probe

Far Field

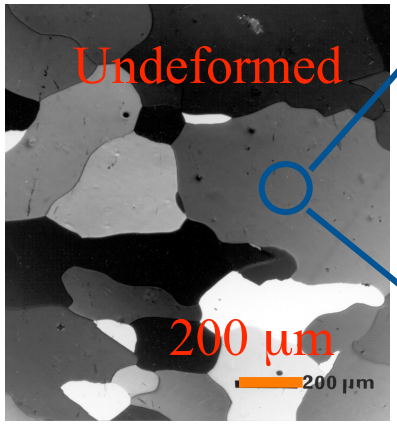

Small deformation

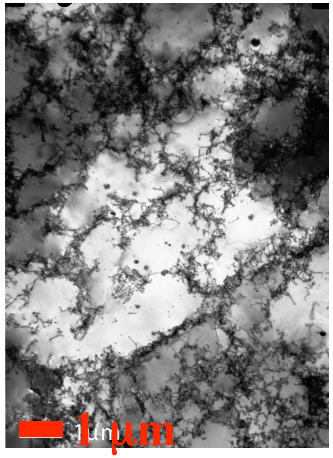

Large deformation

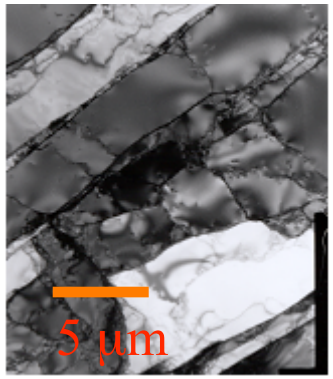

RISØ

Metal Structures in 4D

Setup at 1-ID

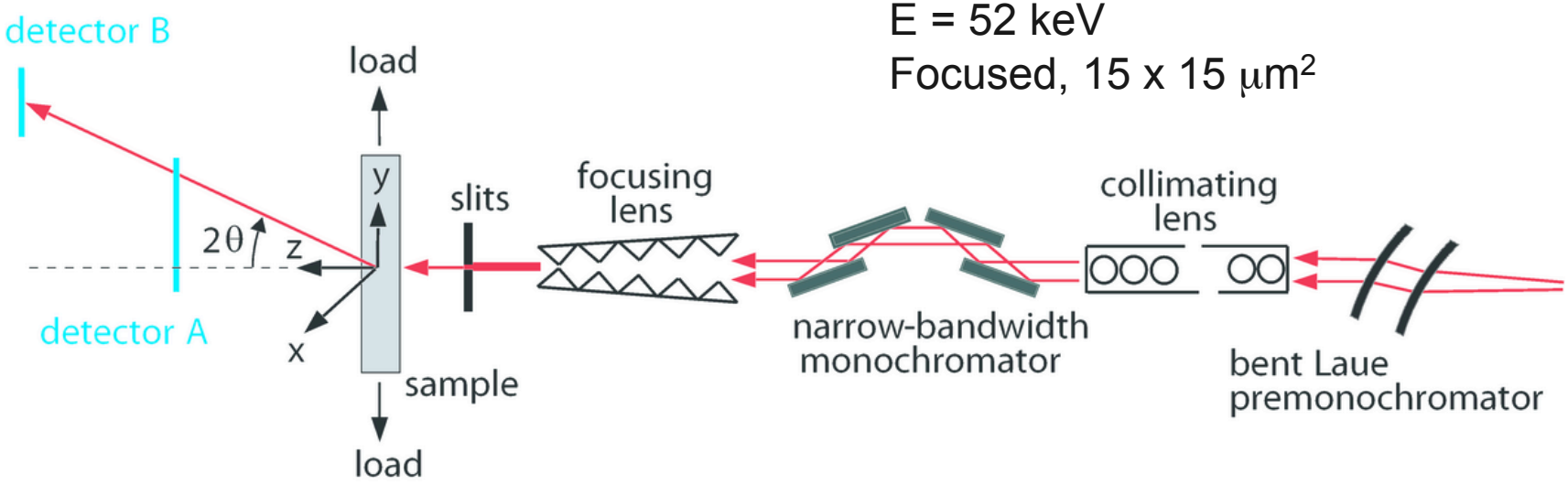

E = 52 keV
Focused, 15 x 15 μm²

Samples

- Cu (99.99% OFHC)
- Cold rolled to 80% reduction, fully recrystallized
- Thickness 300 μm, 30 μm grain size (EBSP)
- Displacement controlled tension rig
- [400] || load axis

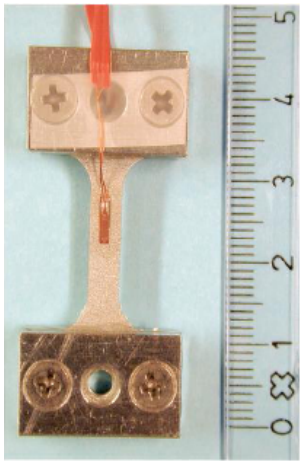

Raw Diffraction Data

Detector A
40 cm from sample

Detector B
4 m from sample

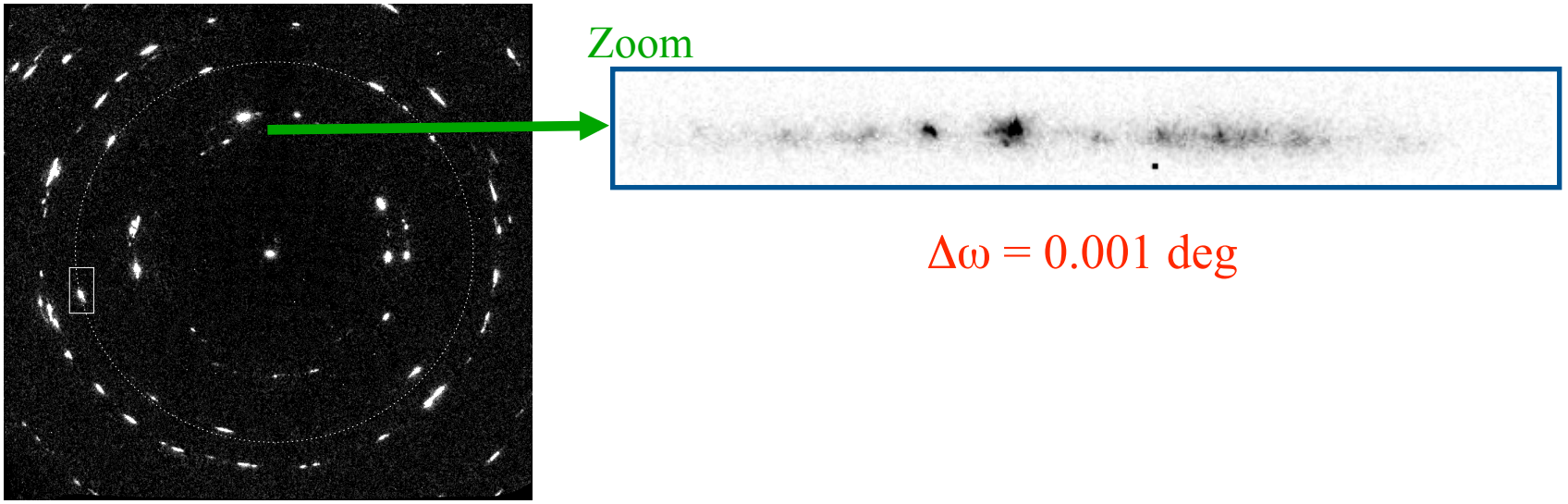

Grain-scale

Subgrain-scale

Cell & wall identification

Strain:

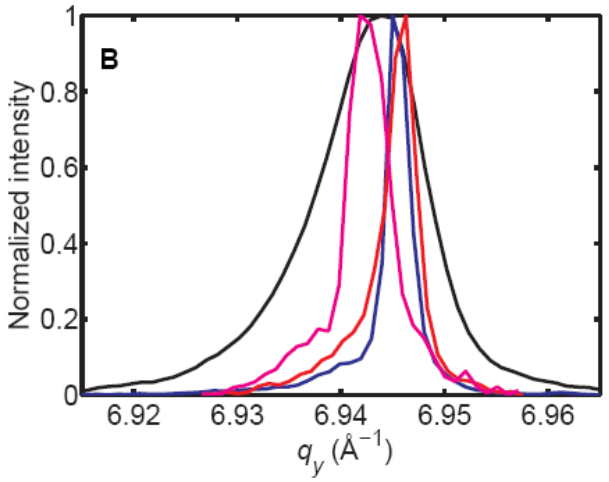

3D reciprocal space map
- 400 Cu at 3.5% strain
- Few minutes acquisition

Subgrains
- Size 1-3 μm
- Sharp peaks from unique sample positions

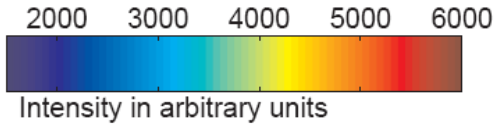

Mosaic spread:

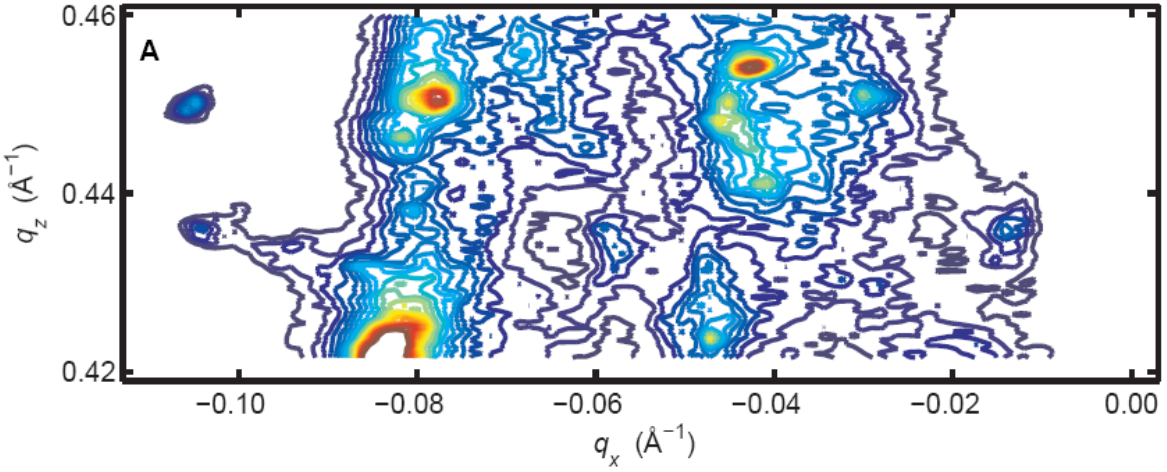

B. Jakobsen et al., *Science* **312** (2006) 889-892

Axial Strain

Cu, (σ || 100)

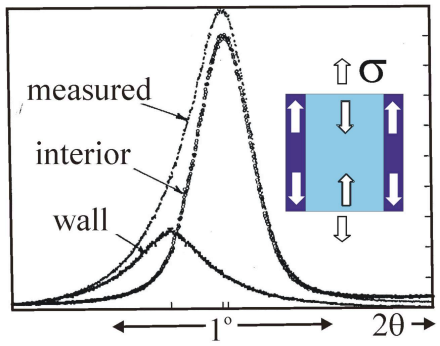

H. Mughrabi, T. Ungár et al., 1980's

- Macroscopic diffraction peak asymmetry
- Dislocation walls: forward stresses
- Dislocation-depleted regions: back stresses
- Each component broadened by respective dislocation density

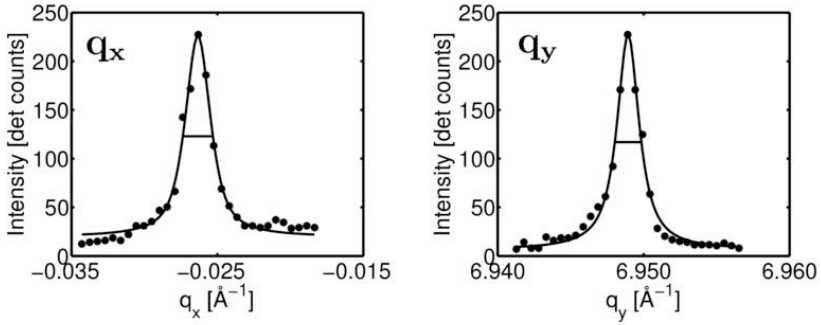

- Subgrains:
  - < 12 dislocations in subgrain
  - Homogeneous internal-strain
  - Strains between subgrains
  - Average back stress
- Dislocation boundary regions
  - Broad diffraction signal
  - Average forward stress

B. Jakobsen et al. (2007) Acta Materialia 55: 3421

Diffraction Tracking

- Grain position, grain boundary topology
- Crystallographic phase & orientation

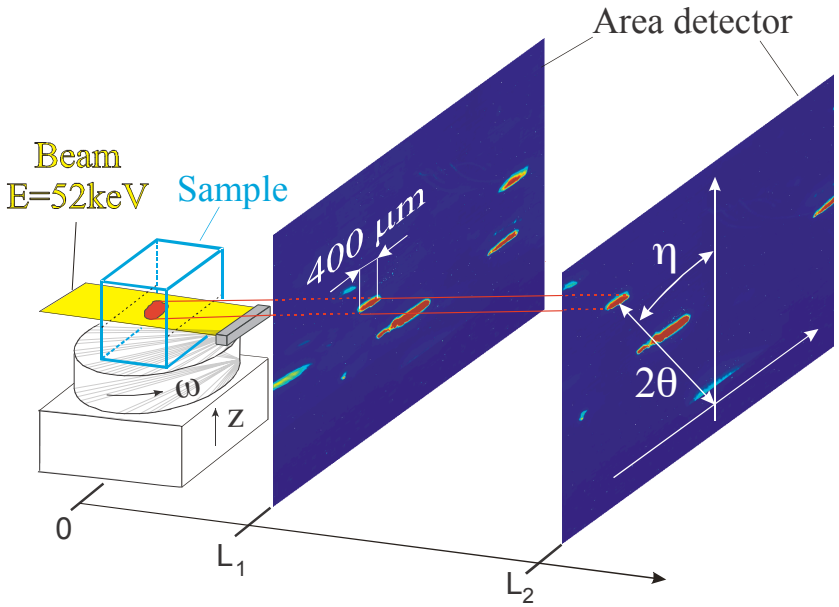

- Grain growth
- Phase transformation
- Initial state before processing

Near Field

- Line focus
- Reflections by ω-rotation
- Projects grain cross section onto detector
- Backtracking => grain outline
- Grain orientation
- Some minutes per layer
- Limitation: mosaic spread

H.F. Poulsen *et al.*, J. Applied Cryst., 2001
R. Suter et al.

Polycrystalline grain maps

- Sample: aluminum 1050 polycrystal
- 500C anneal for 50 minutes
- EDM cut cylinder of about 1 mm diameter
- Data acquisition time per layer ≈ 30 min

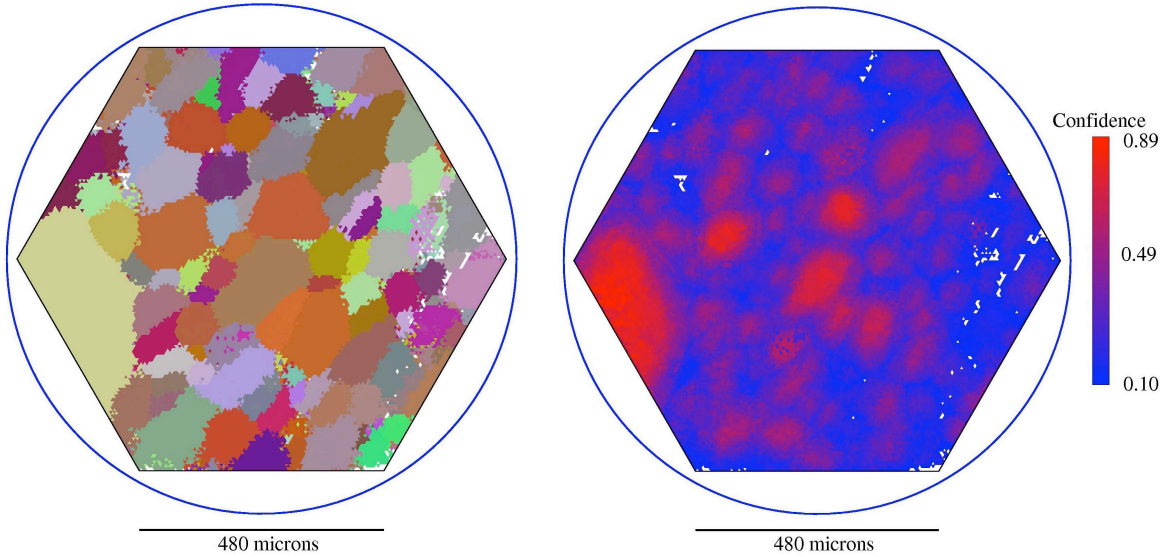

3D rendering
from 6 slices

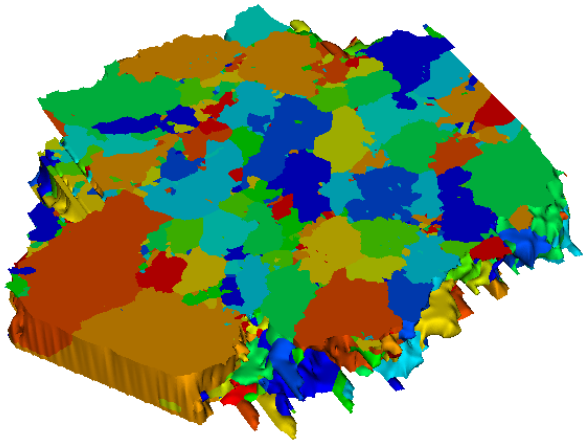

- ~24,500 triangular area elements
- Number of qualified Bragg peaks: 35 - 4
- Parallel algorithm implemented (B. Tieman, APS)

R.H. Moore, et al,
Comp. Mat. Sci.

Example 3: Layered System

Multiple requirements for functionality

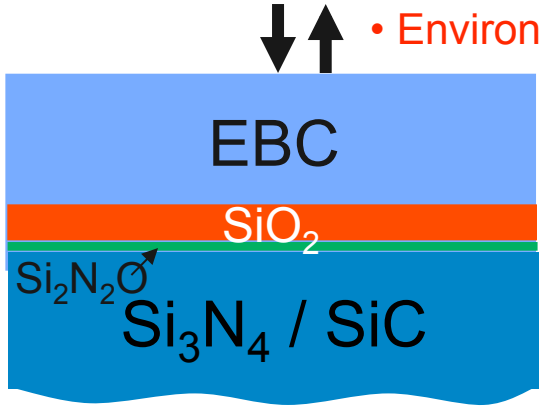

- Environmental integrity
- Chemical compatibility
- Thermal mismatch
- Phase stability

Coating growth conditions often lead to non-equilibrium microstructures

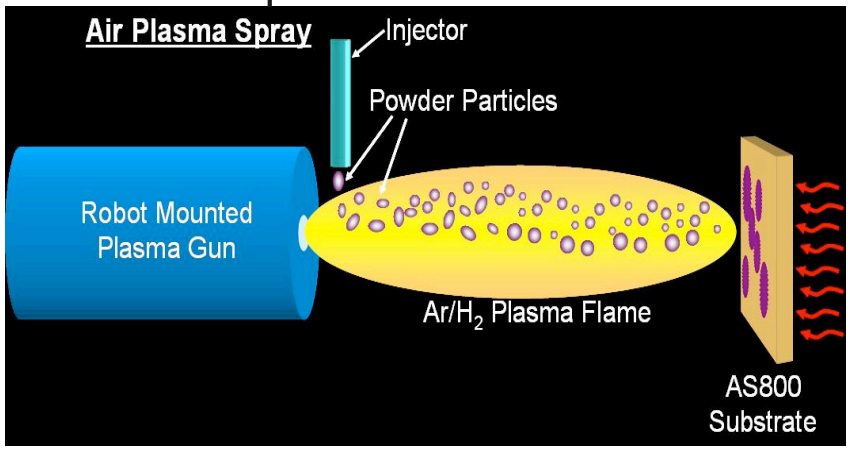

SOFC

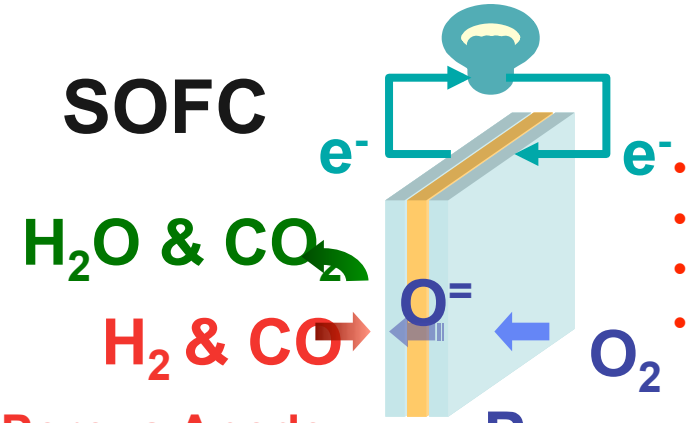

- Controlled porosity
- Thermal mismatch
- Chemical durability
- Mechanical integrity

Investigate

- intra-layer microstructure
- inter-layer effects

Work of J. Almer

High-energy microfocusing to study layered systems

side view

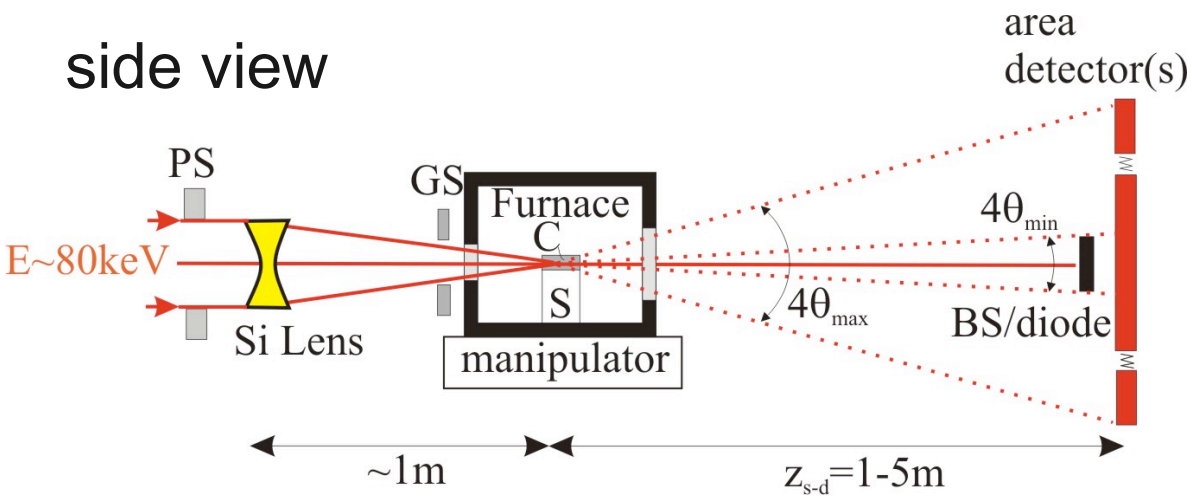

2-d view

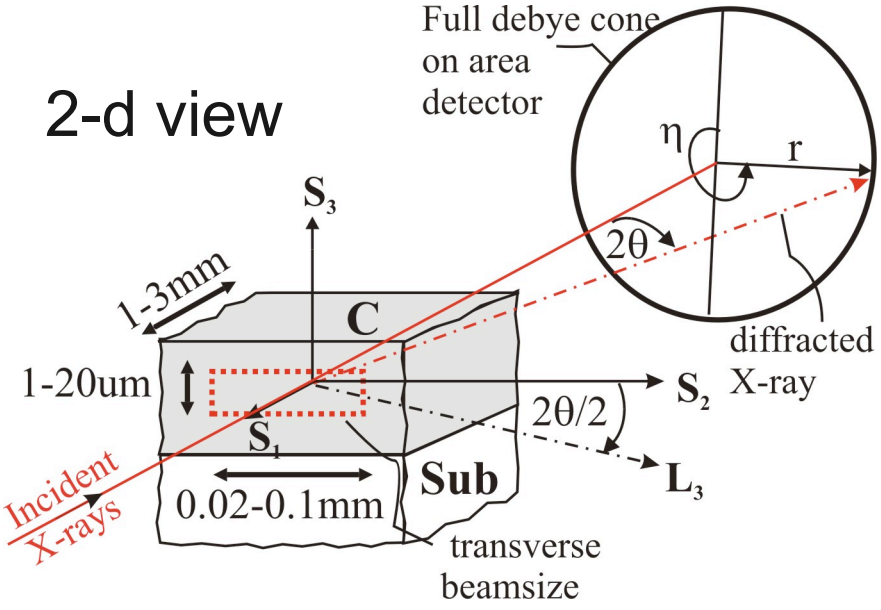

Key features

- Focus vertical size to ~1um with sufficiently small divergence (~100urad)
- WAXS/SAXS/radiography on same sample volume
- High sample & chamber penetration power

- Small bragg angles – measure nearly along 2 principal sample directions
- Coatings typically isotropic in-plane: unique information in single exposure
- Direct depth resolution (cf. cumulative in reflection geometry)

Solid-oxide fuel cells – Cr poisioning

Use of a metallic interconnect is a key to optimize SOFC efficiency & cost…

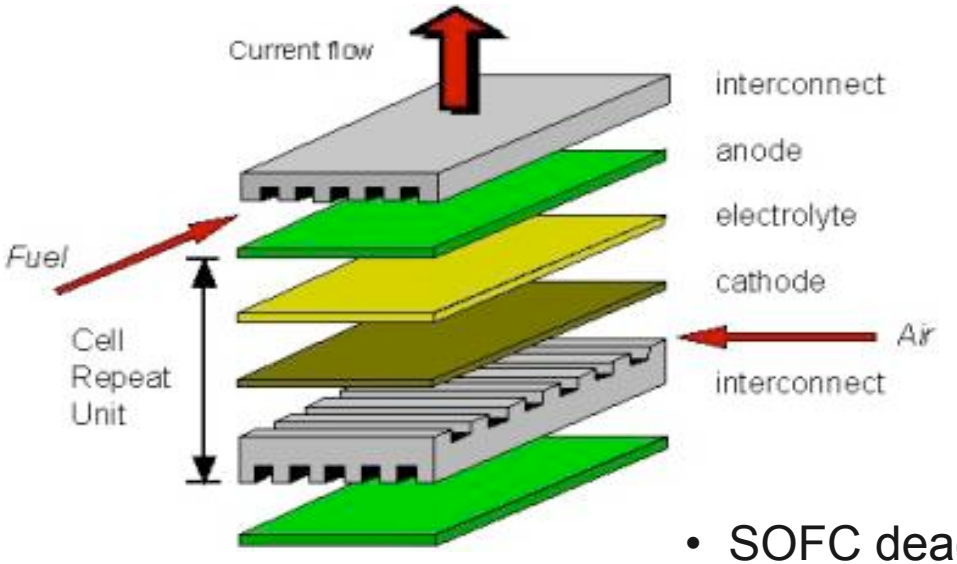

BUT susceptible to Cr poisoning

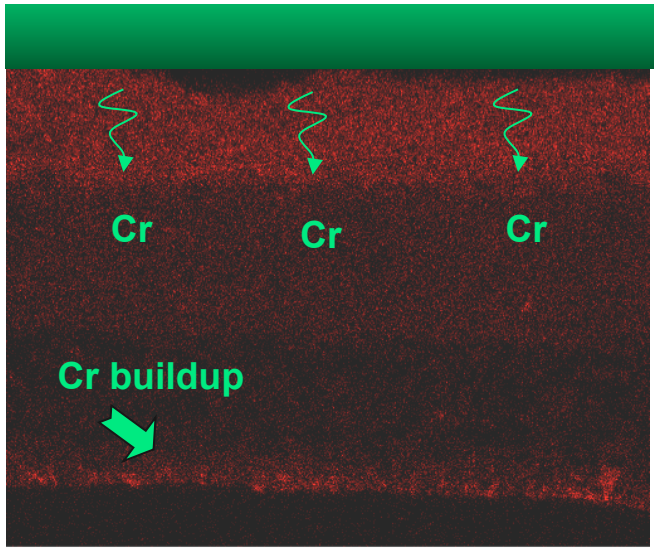

Cr Ka1

- SOFC deactivation is often associated with Cr accumulation -> from metallic interconnect
- Knowledge of different Cr species & distribution is critical for understanding the deactivation mechanism
- Past experiments limited to imaging (SEM, EDX), inconclusive in separating phase & distribution
- Conventional XRD method lacks spatial resolution and sensitivity

SOFC testing and microstructure

Cut 1mm cross-section from center

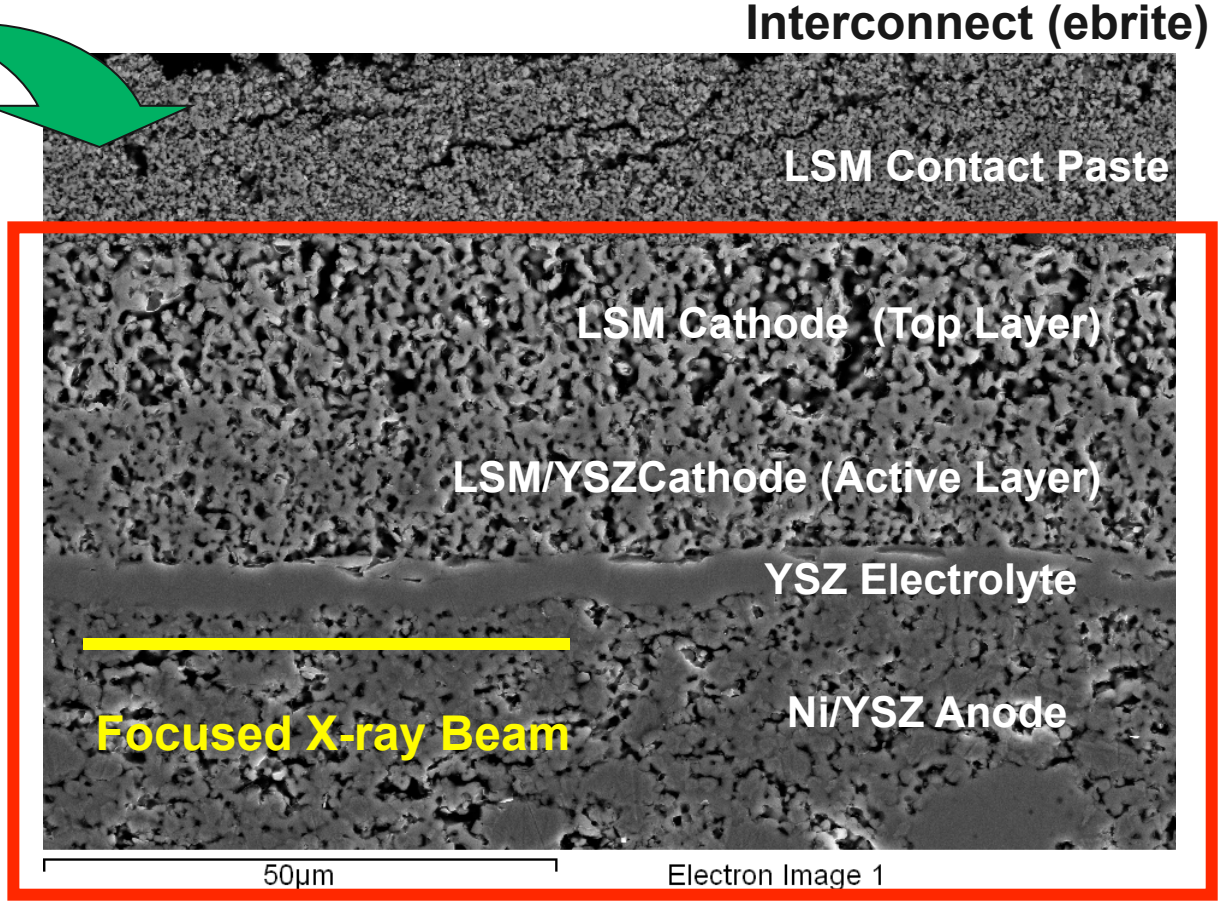

SEM Image of InDec SOFC Cross-section

Button-cell testing

- Current Density 250 mA/cm^2
- Air /fuel Flow 70/400 sccm
- T=800C
- Cell voltage to 0 (de-activation) after ~110hr test time

SOFC diffraction data and analysis

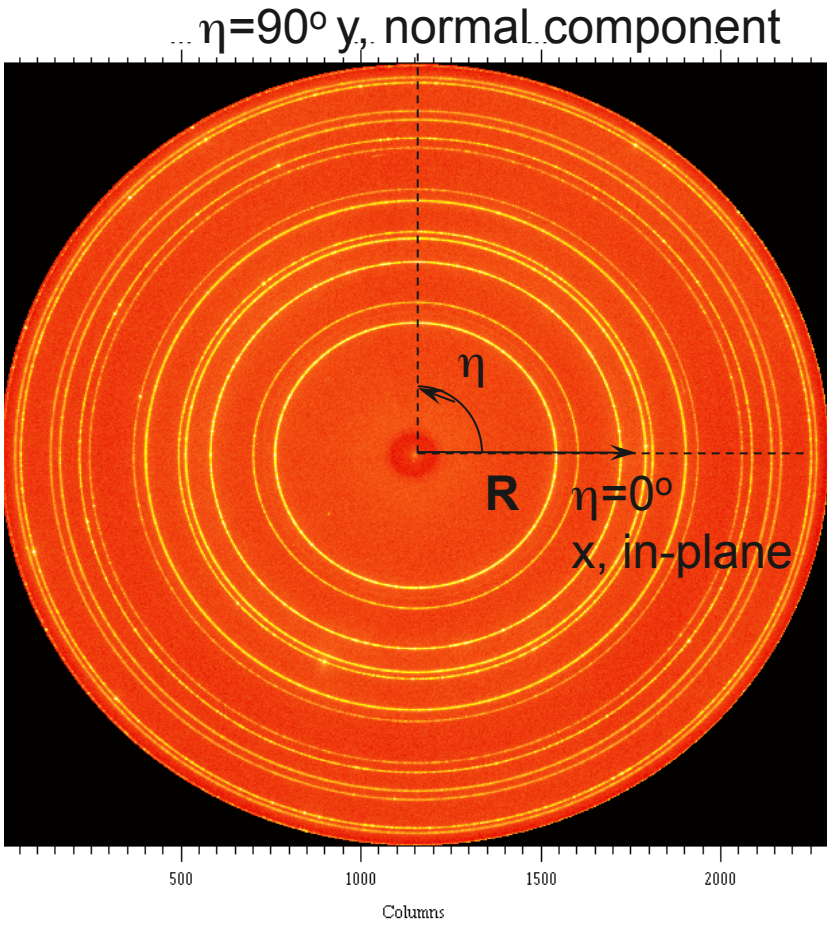

Typical pattern (multiple phases)
Mar345, E=80.7 keV

Intensity

- Smooth & constant vs η (fine grained, no texture)
- Reliable Reitveld phase fractions (w_i)

Radius versus azimuth

- deviatoric strain
- $\Delta\varepsilon = -(r_{xx} - r_{yy})/r_{mean}$

Mean radius

- Reitveld -> lattice parameters
- stoichiometry

Sample transmission & phase fractions

- Integrated porosity

$$P_{\text{int}} = \frac{z_{sam} - z_{eff}}{z_{sam}}$$

$$z_{eff} = \frac{-\ln(T)}{\sum_{i=1}^{N} w_i \mu_i}$$

SOFC phase, porosity, strain & Ip maps

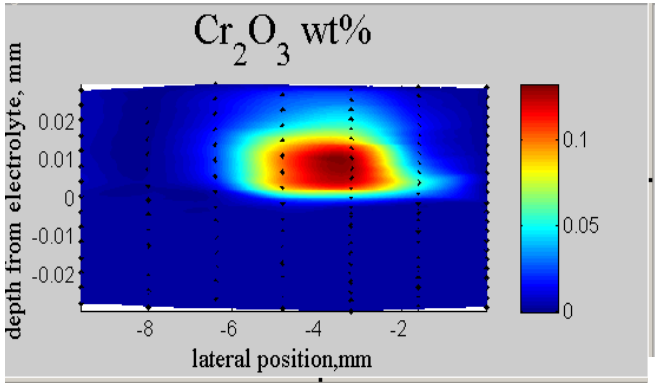

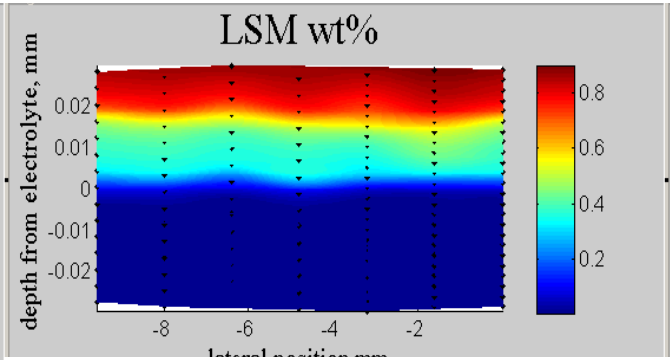

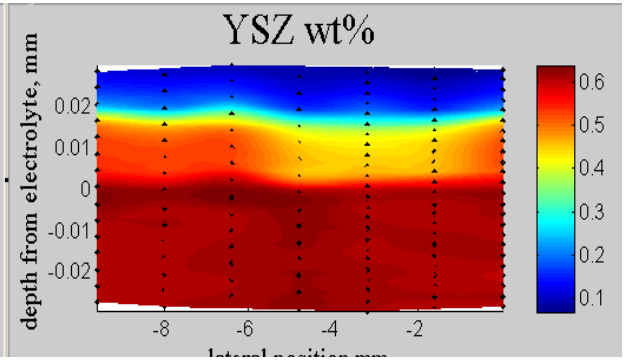

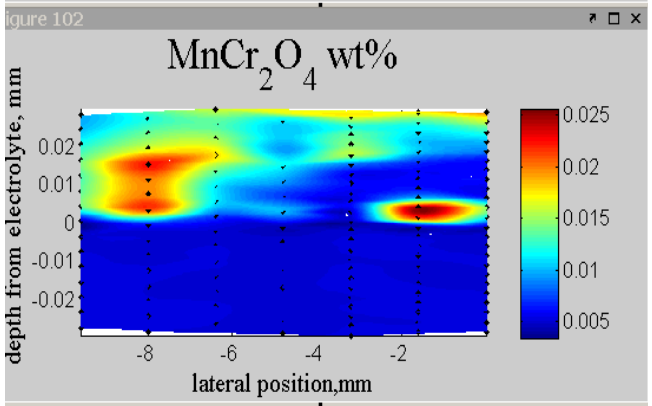

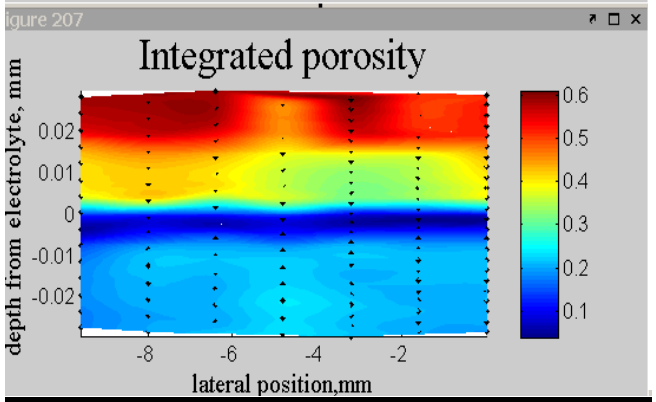

- Transition between 2 Cr phases in "active cathode" region
- Cr_2O_3 built up at cathode/electrolyte interface
  - Lateral dependence with current collector position
    - *suggests formation through electrochemical reduction*
  - Associated with decreased cathode porosity -> mass transfer of Cr
    - *Plays role in decreasing percolation -> increasing impedance*
- Cr/Mn spinel has weaker spatial association
    - *suggests chemical process (Cr gas transport & solid diffusion)*

Proposed mechanism of Cr poisoning

Cr Accumulation Mechanism

- Generation at metallic interconnect

$$Cr_2O_3(s) + 1.5O_2(g) + 2H_2O(g) = 2CrO_2(OH)_2(g)$$

- **Deposition through Electrochemical Process**[1]

$$2CrO_2(OH)_2(g) + 6\,e^- = Cr_2O_3(s) + 2H_2O(g) + 3O^{2-}$$

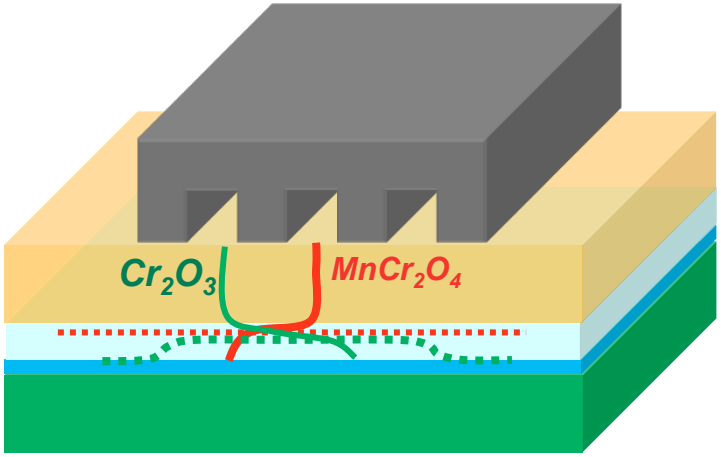

- Deposition through Chemical Process[2]

$$3CrO_2(OH)_2(g) + La_{1-x}Sr_xMnO_3(s) = La_{1-x}Sr_xCrO_3(s) + MnCr_2O_4(s) + 3H_2O(g) + 2.5O_2$$

1. K. Hilpert, D. Das, M. Miller, D. H. Peck and R. Weiß, *J. Electrochem. Soc.* **143**, 3642, 1996
2. S. P. S. Badwal, R. Deller, K. Foger, Y. Ramprakash, J. P. Zhang, *Solid State Ionics*, **99**, 297, 1997

Studies of layered systems at 1-ID

- Environmental barrier coatings
  - Ta_2O_5 (with Al_2O_3 and La_2O_3) on Si_3N_4 (J. Almer, K. Faber, C. Weyant, K. Lee)
  - Mullite/Barium-Strontium Aluminosilicate on Si/SiC (J. Almer, K. Faber, B. Harder)
- Thermal barrier coatings
  - Depth-resolved phase, strain and porosity (SAXS/WAXS) of EB-PVD TBCs
    - *A. Kulkarni, H. Herman, J. Almer et al, J. Am. Cer. Soc 87, p. 268-74 (2004).*
  - In-situ oxidation studies of phase and strain evolution on TBC bondcoat
    - *J. Almer, E. Ustundag, G.Swift, J.Nycha and D. Clarke, Mat. Sci. Forum 490, p.287-93 (2005)*
  - Localized strain measurements in plasma-sprayed TBCs
    - *J. Thornton, S. Slater and J. Almer, J. Am. Cer. Soc. 88(10), p. 2817-2825 (2005).*
- Metal-nitride coatings
  - Strain, texture and phase-decomposition analysis (SAXS/WAXS)
    - *J. Almer, U. Lienert, R. Peng, C. Schlauer and M. Oden, J. App. Physics 94, p. 697-702 (2003).*
    - *M. Terner, P. Hedstrom, J. Almer, J. Ilavsky and M. Oden, Mat. Sci. Forum 524, p. 619-624 (2006)*
- Solid-oxide fuel cells
  - Depth-resolved porosity and phase analysis (SAXS/WAXS)
    - *A. Allen, T. Dobbins, F. Zhao, J. Ilavsky, J. Almer and F. DeCarlo, Cer. Eng. 25(3), p. 275-80 (2004).*
  - Investigation of Cr-poisoning mechanism (J. Almer, D. J. Liu)

Conclusions/Comments

- The use of high energy x-rays present many new experimental possibilities for the study of materials.
- Stress/strain/texture can be studied in a wide variety of materials using both aggregate and single grain methods.
- Data from these experiments can help to verify/reject results from modeling.
  - We are always looking to establish better connections to theorists and modelers.
- More and more, these studies are being done under “real time” conditions to monitor materials evolution during processing, etc.
- Use of a combination of methods is a powerful methodology
  - Fuel cells as one example
- Improvements in undulators and x-ray optics will provide substantial gains x-ray flux density in the near future, providing exciting new capabilities.

Who: Acknowledgements

- 1-ID Personnel
  - **Jon Almer**
  - **Ulrich Lienert**
  - Peter Lee
  - Sarvjit Shastri
  - Ali Mashayekhi
- Students
  - **Marcus Young** (steel)
    - *Now at Ruhr Univ. (Bochum)*
  - Alix Deymier (NU, bone/teeth)
  - Anjali Singhal (NU, bone)
  - Fang Yuan (NU, bone)
- Collaborators
  - David Dunand (Northwestern)
  - Cate Brinson (Northwestern)
  - Robert Suter (Carnegie Mellon)
  - Stuart Stock (Northwestern Medical)
  - Henning Poulsen (Risø)
  - Wolfgang Pantleon (Risø)

Funding by the Department of Energy, Basic Energy Sciences